전자파 차폐/흡수 소재 측정 기술

Prof. Hyun Ho Park
hhpark@suwon.ac.kr
Dept. Electronic Engineering
The University of Suwon

August 23, 2023

Contents

소재의 전자파 차폐 및 흡수 원리

Prof. Hyun Ho Park
hhpark@suwon.ac.kr
Dept. Electronic Engineering
The University of Suwon

Source and Medium

- 필드의 특성은 소스, 매질, 소스와 관측지점 간의 거리에 의해 결정
- 소스 근처의 필드 특성은 주로 <u>소스 특성에 의해 결정</u>
- 먼 곳의 필드 특성은 주로 <u>매질에 의존</u>

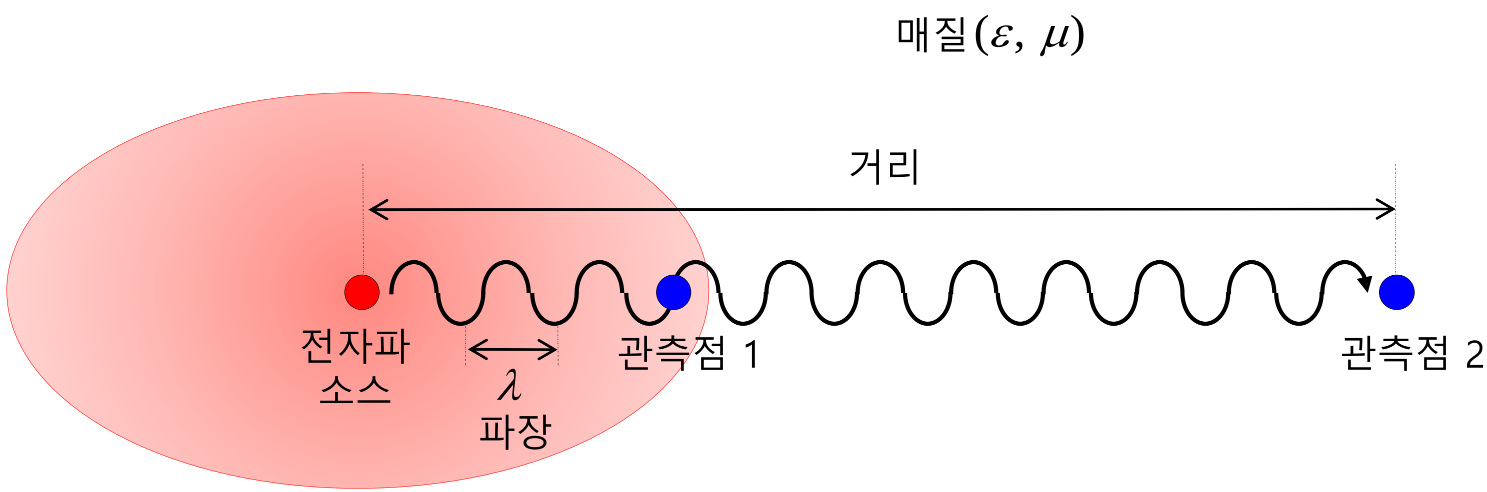

EMC Sources

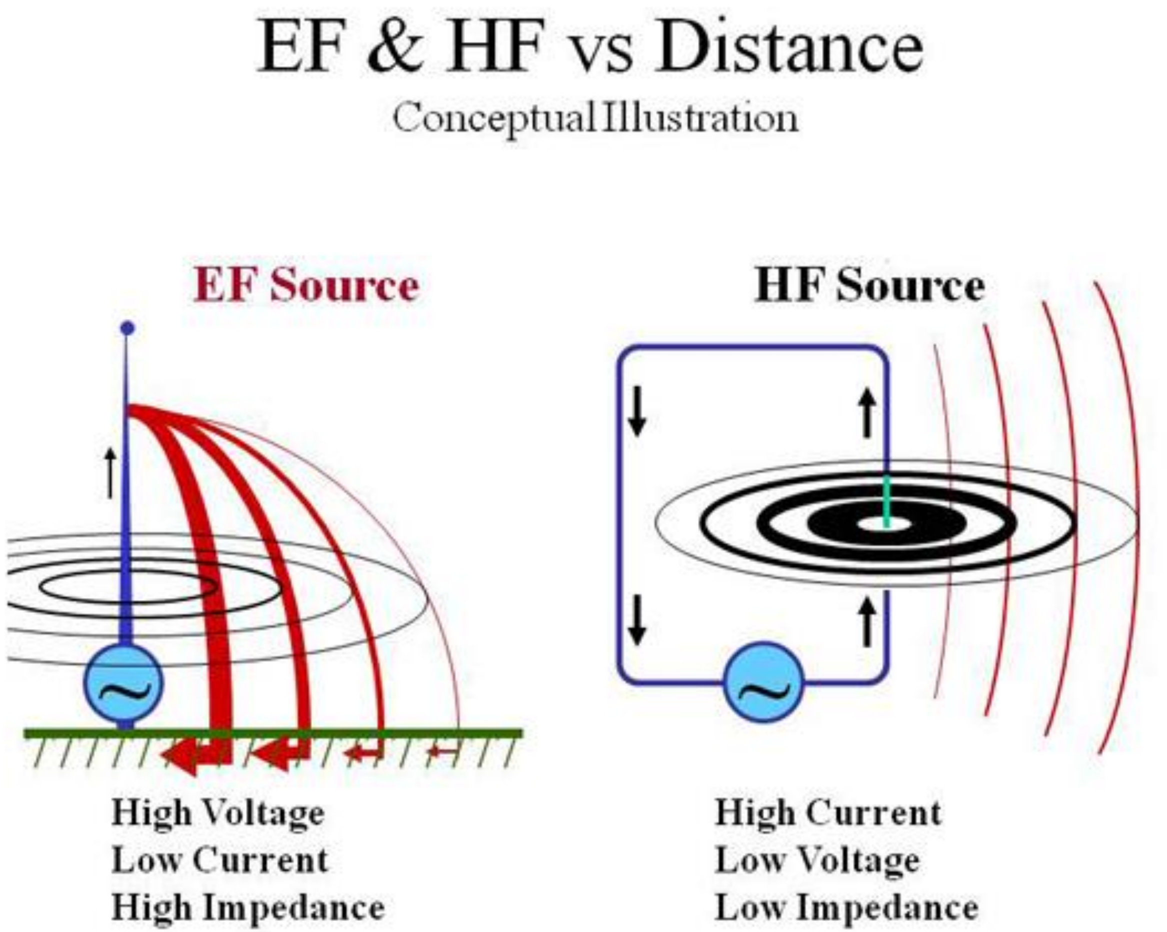

https://interferencetechnology.com/designing-rf-shielded-enclosure/#

Electromagnetic Sources

- **Electric Dipole Radiation**

$$E_\theta = \eta_0 \frac{Idl}{4\pi}\beta_0^2 \sin\theta \left[j\frac{1}{\beta_0 r} + \frac{1}{\beta_0^2 r^2} - j\frac{1}{\beta_0^3 r^3} \right] e^{-j\beta_0 r}$$

$$H_\phi = \frac{Idl}{4\pi}\beta_0^2 \sin\theta \left[j\frac{1}{\beta_0 r} + \frac{1}{\beta_0^2 r^2} \right] e^{-j\beta_0 r}$$

- **Magnetic Dipole Radiation**

$$E_\phi = -j\frac{\omega\mu_0 m}{4\pi}\beta_0^2 \sin\theta \left[j\frac{1}{\beta_0 r} + \frac{1}{\beta_0^2 r^2} \right] e^{-j\beta_0 r}$$

$$H_\theta = j\frac{\omega\mu_0 m}{4\pi\eta_0}\beta_0^2 \sin\theta \left[j\frac{1}{\beta_0 r} + \frac{1}{\beta_0^2 r^2} - j\frac{1}{\beta_0^3 r^3} \right] e^{-j\beta_0 r}$$

- **전자파 소스가**
  - 낮은 전류/높은 전압을 갖는다면 전기적 특성이 우세
    ex) Pole antenna
  - 높은 전류/낮은 전압을 갖는다면 자기적 특성이 우세
    ex) Loop antenna

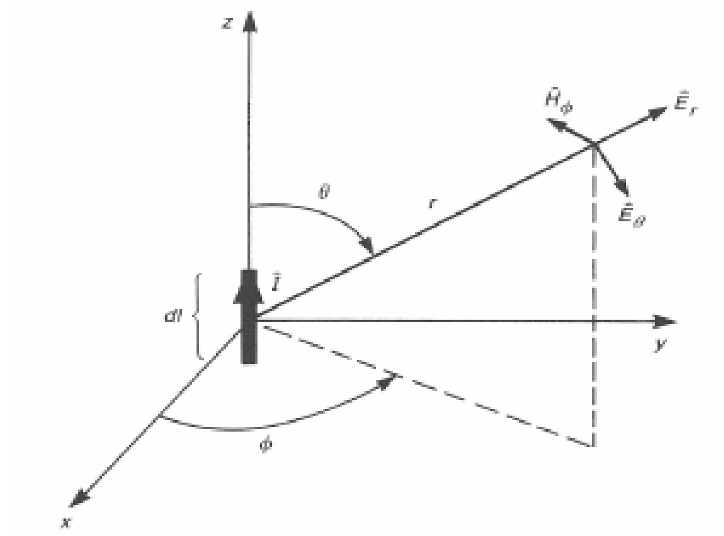

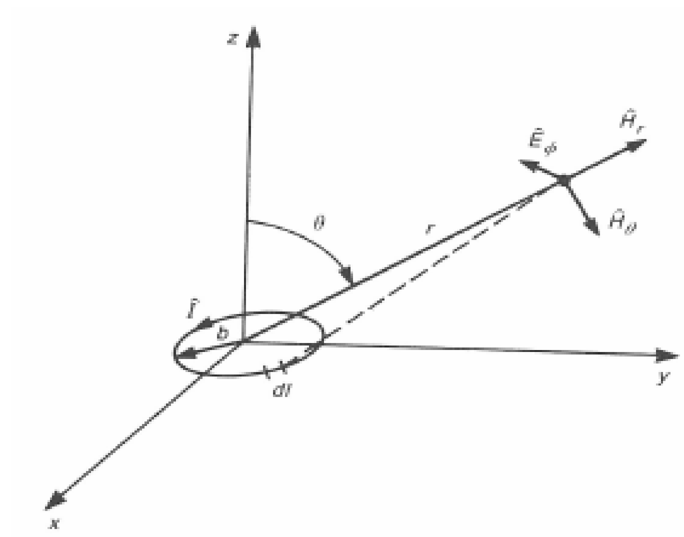

Far-field/Near-field

➢ **Far-field (** $\beta_0 r >> 1;\ r >> \lambda/2\pi$ **)**

- **Electric Dipole Radiation**

$$E_\theta = j\eta_0 \frac{Idl}{4\pi}\beta_0^2 \sin\theta \frac{1}{\beta_0 r} e^{-j\beta_0 r}$$

$$H_\phi = j\frac{Idl}{4\pi}\beta_0^2 \sin\theta \frac{1}{\beta_0 r} e^{-j\beta_0 r}$$

$$\frac{E_\theta}{H_\phi} = \eta_0$$

- **Magnetic Dipole Radiation**

$$E_\phi = \frac{\omega\mu_0 m}{4\pi}\beta_0^2 \sin\theta \frac{1}{\beta_0 r} e^{-j\beta_0 r}$$

$$H_\theta = -\frac{\omega\mu_0 m}{4\pi\eta_0}\beta_0^2 \sin\theta \frac{1}{\beta_0 r} e^{-j\beta_0 r}$$

$$\frac{E_\theta}{H_\phi} = \eta_0$$

➢ **Near-field (** $\beta_0 r << 1;\ r << \lambda/2\pi$ **)**

- **Electric Dipole Radiation**

$$E_\theta = -j\eta_0 \frac{Idl}{4\pi}\beta_0^2 \sin\theta \frac{1}{\beta_0^3 r^3} e^{-j\beta_0 r}$$

$$H_\phi = \frac{Idl}{4\pi}\beta_0^2 \sin\theta \frac{1}{\beta_0^2 r^2} e^{-j\beta_0 r}$$

$$\frac{E_\theta}{H_\phi} = \frac{\eta_0}{\beta_0 r} > \eta_0$$

- **Magnetic Dipole Radiation**

$$E_\phi = -j\frac{\omega\mu_0 m}{4\pi}\beta_0^2 \sin\theta \frac{1}{\beta_0^2 r^2} e^{-j\beta_0 r}$$

$$H_\theta = \frac{\omega\mu_0 m}{4\pi\eta_0}\beta_0^2 \sin\theta \frac{1}{\beta_0^3 r^3} e^{-j\beta_0 r}$$

$$\frac{E_\theta}{H_\phi} = \eta_0 \beta_0 r < \eta_0$$

Far-field/Near-field

- 필드 공간을 두 영역으로 나눌 수 있다

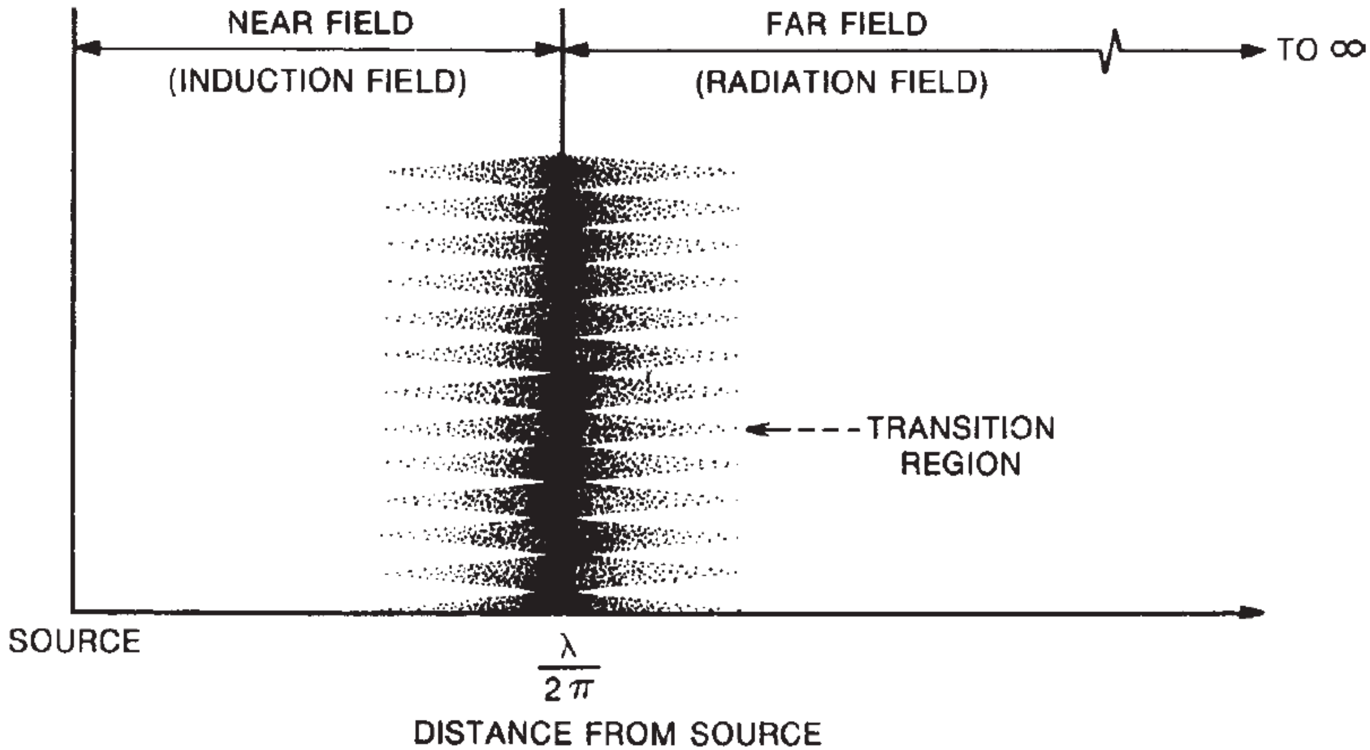

Source : H. W. Ott, Electromagnetic Compatibility Engineering, Wiley, 2009

Wave Impedance

- 전기장(E)과 자기장(H)의 비율
  - **Far field** 에서 파동 임피던스 = 공기 혹은 자유공간의 임피던스
  - **Near field**에서 파동 임피던스는 소스의 특성과 관측 지점까지의 거리에 의해 결정

$$\eta_0 = \frac{E}{H}$$

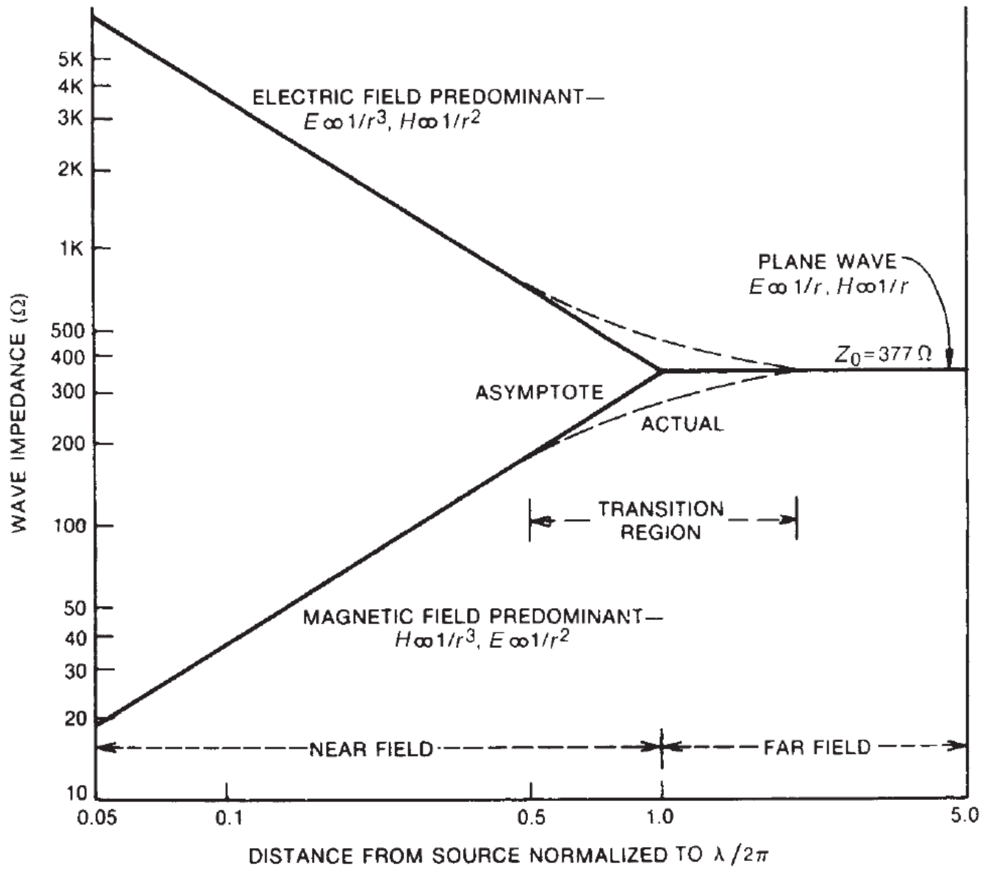

Source : H. W. Ott, Electromagnetic Compatibility Engineering, Wiley, 2009

Shielding Effectiveness

- 차폐는 쉴드에 의한 자기장 혹은 전기장 감소라고 명시될 수 있음

- 차폐 효과의 표현 식
  - $S = 20\log\frac{E_0}{E_1}$ dB (전기장)
  - $S = 20\log\frac{H_0}{H_1}$ dB (자기장)
  - 여기서, $E_0(H_0)$ 는 입사파의 세기, $E_1(H_1)$는 투과파의 세기

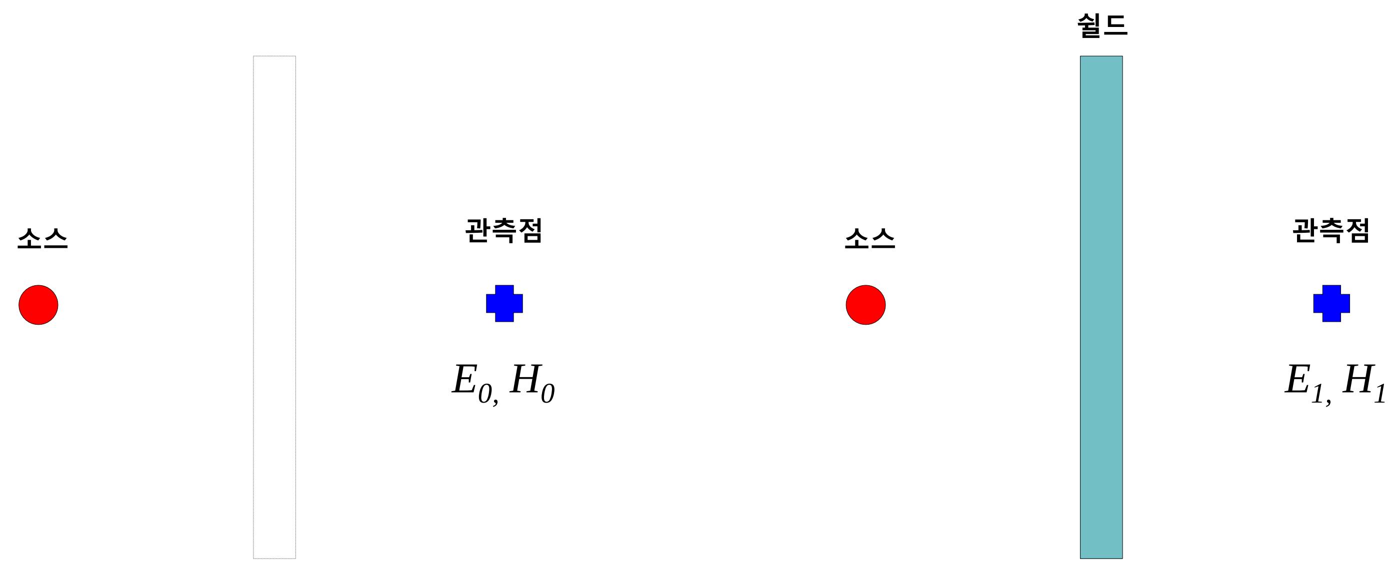

Shielding Effectiveness

- 차폐 효과 : S = A + R + B (dB)
  - 흡수 손실 (A) : 표면을 투과한 파가 매질을 통과함에 따라 감쇠
    - Near-field/Far-field 그리고 전기장/자기장과 무관
  - 반사 손실 (R) : 표면으로부터 부분적으로 반사되어 나타나는 손실
    - 필드 유형과 임피던스에 의존
  - Multiple Reflection 보정 계수 (B)

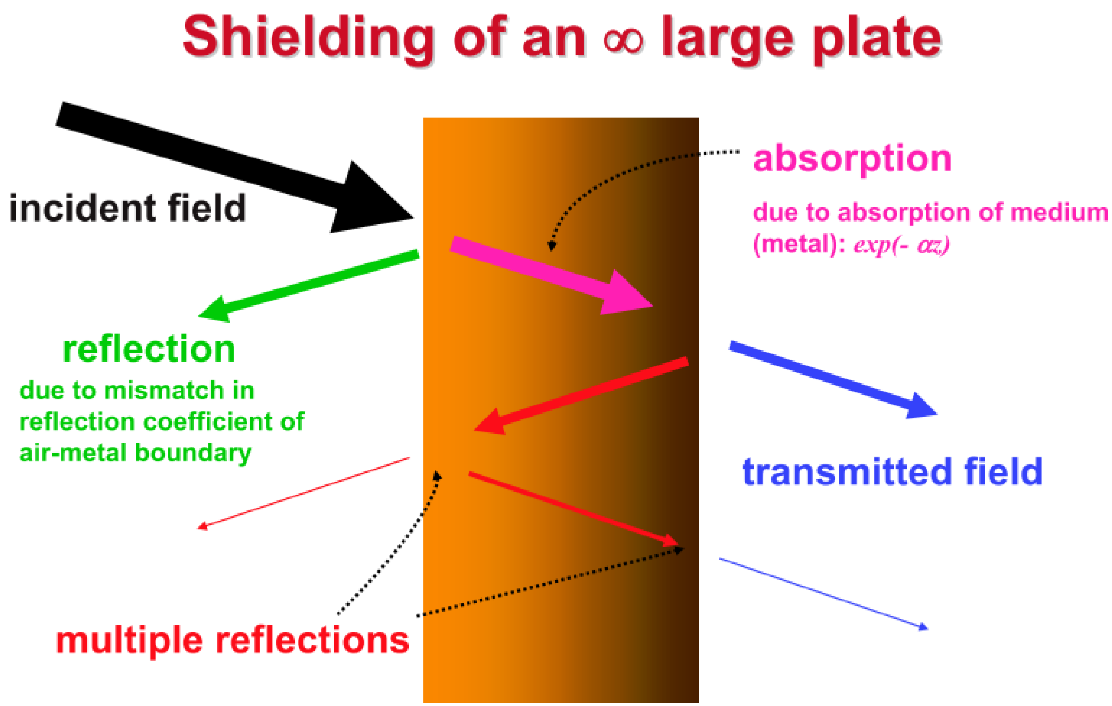

Source : F. Leferink, IEEE EMC Symposium 2010, Fort Lauderdale, Tutorial on EMC Fundamentals; Shielding

Reflection/Transmission

- 전파가 두 개의 경계면을 통과하는 경우, 두 번째 경계를 통과하는 투과파
  - $E_t = \frac{2Z_1}{Z_1+Z_2} E_1$, $H_t = \frac{2Z_2}{Z_1+Z_2} H_1$
- 쉴드가 **skin depth**와 비교하여 두꺼운 경우, 전체 투과파 세기
  - $E_t = \frac{4Z_1Z_2}{(Z_1+Z_2)^2} E_0$, $H_t = \frac{4Z_1Z_2}{(Z_1+Z_2)^2} H_0$

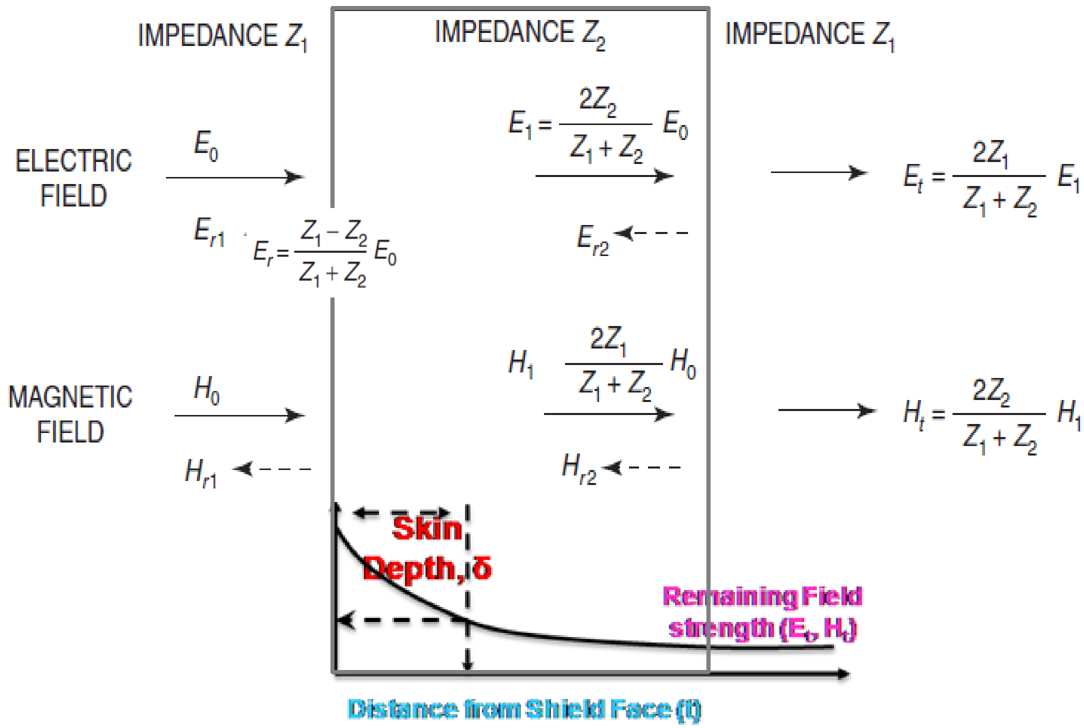

차폐재의 총 투과계수 :

$$T_t = \frac{2Z_2}{Z_2 + Z_1} \cdot \frac{2Z_1}{Z_2 + Z_1} = \frac{4Z_1Z_2}{(Z_2 + Z_1)^2}$$

Source : H. W. Ott, Electromagnetic Compatibility Engineering, Wiley, 2009

Reflection/Transmission

- $Z_1 \gg Z_2$ 인 경우
  - 전기장이 쉴드로 들어갈 때 (첫 번째 경계) 가장 큰 반사 발생
    - 아주 얇은 물질도 좋은 반사 손실을 제공
    - $E_t = \frac{4Z_2}{Z_1} E_0$
  - 자기장이 쉴드로 들어갈 때 (두 번째 경계) 가장 큰 반사 발생
    - 쉴드 내에서의 multiple reflection 은 쉴드 효과를 감소시킴
    - $H_t = \frac{4Z_2}{Z_1} H_0$

$$Z_1 >> Z_2$$

$$T_t = \frac{4Z_1Z_2}{(Z_2+Z_1)^2} \approx \frac{4Z_2}{Z_1}$$

- **So we can conclude that**
  - **Reflection attenuation for the electric component is independent of the thickness of the material of the conducting plate**
  - **Reflection attenuation for the magnetic component is influenced by the thickness of the material,**
- **Simplified:**
  - **Shielding of electric field component via reflection,**
  - **Shielding of magnetic field component via absorption**

- 만약 $Z_1 = Z_w$, $Z_2 = Z_s$이면 multiple reflection을 무시한 반사 손실을 얻을 수 있음

- $R = 20log \frac{|Z_w|}{4|Z_s|} \quad (dB)$
  - Z_w: 쉴드로 들어가기 전의 파동 임피던스
  - Z_s: 쉴드의 임피던스

Plane Wave Reflection Loss

- 평면파에 대한 반사 손실
  - 평면파의 경우, 파동 임피던스 Z_w = 자유 공간의 특성 임피던스 Z_o
    - $R = 20\log\frac{94.25}{|Z_s|}\ (dB)$
    - 쉴드 임피던스가 감소할수록 반사 손실이 증가

  - 도체의 경우 ($\sigma \gg j\omega\epsilon$) 특성 임피던스 = 쉴드 임피던스
    - $Z_o = \sqrt{\frac{j\omega\mu}{\sigma+j\omega\epsilon}}$, $Z_s = \sqrt{\frac{j\omega\mu}{\sigma}} = \sqrt{\frac{\omega\mu}{2\sigma}}(1+j)$: 도전성 차폐재의 임피던스 수식
    - $|Z_s| = \sqrt{\frac{\omega\mu}{\sigma}} = 3.68\times10^{-7}\sqrt{\frac{\mu_r}{\sigma_r}}\sqrt{f}$

μ_r : 공기 대비 비 투자율

σ_r : Copper 대비 비 도전율

  - 따라서 반사 손실은 다음과 같이 정리할 수 있음
    - $R = 168 + 10\log(\sigma_r/\mu_r f)\ (dB)$

☞ **So the reflection term is**
- **large for low frequencies**
- **reduces with the square root of the frequency, 10dB/dec**

Plane Wave Reflection Loss

- 세 가지 물질 (Copper, Aluminum, Steel) 에 대한 반사 손실 그래프
- Copper 와 Aluminum이 Steel 보다 반사 손실은 크다

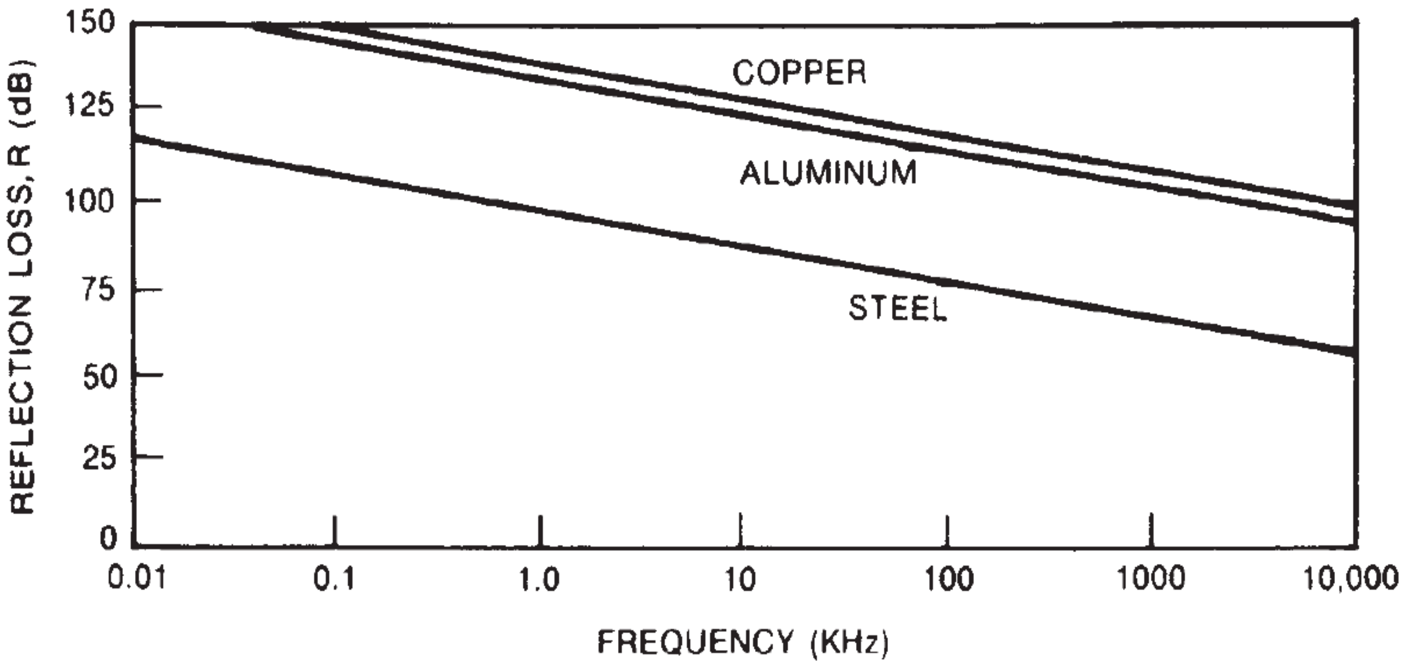

Source : H. W. Ott, Electromagnetic Compatibility Engineering, Wiley, 2009

Absorption Loss

- 전자파가 임의의 매질을 통과하면, 매질에 유도된 전류가 저항 손실과 열을 생성
  - $E_1 = E_0 e^{-t/\delta}$, $H_1 = H_0 e^{-t/\delta}$
  - 여기서, $E_1(H_1)$는 매질 내 임의의 거리 t에서 전파 세기
- 전파가 원래 세기의 약 37%로 감쇠되기 위해 요구되는 거리가 skin depth라고 정의됨

$$\boxed{\delta = \sqrt{\frac{2}{\omega\mu\sigma}}\ (m) = \delta = \frac{2.6}{\sqrt{f\mu_r\sigma_r}}\ (in)}$$

TABLE 20.1 Skin depth (δ) for some common materials

Material	$f = 60$ Hz	$f = 10^3$ Hz	$f = 10^6$ Hz	$f = 10^9$ Hz
Copper	8.61 mm	2.1 mm	0.067 mm	2.11 μm
Iron	0.65 mm	0.16 mm	5.03 μm	0.016 μm

- 쉴드를 통과하는 흡수 손실
  - $A = 20\left(\frac{t}{\delta}\right)\log(e)\ (dB) = 8.69\left(\frac{t}{\delta}\right)\ (dB)$ $\longleftarrow$ $SE = 20\log\left|\frac{E_0}{E_t}\right| = 20\log(e^{t/\delta})$
  - 쉴드의 두께 t가 skin depth와 같다면 흡수 손실은 약 9dB
- t/δ 대비 dB 단위 흡수 손실 그래프
  - 평면파, 전기장, 자기장에 적용 가능

Absorption Loss

- Copper와 steel의 서로 다른 두 두께에 대한 주파수 대비 흡수 손실 그래프
- 얇은 (0.02in) copper sheet
  - 1MHz에서 상당한 흡수 손실 (66dB) 발생
  - 1kHz 이하 주파수에서는 손실이 거의 없음
- 흡수 손실 제공 측면에서 steel이 copper보다 우세함
- Steel이 사용되는 경우, 1kHz 이하에서 큰 흡수 손실을 제공하기 위해 두꺼운 sheet 필요

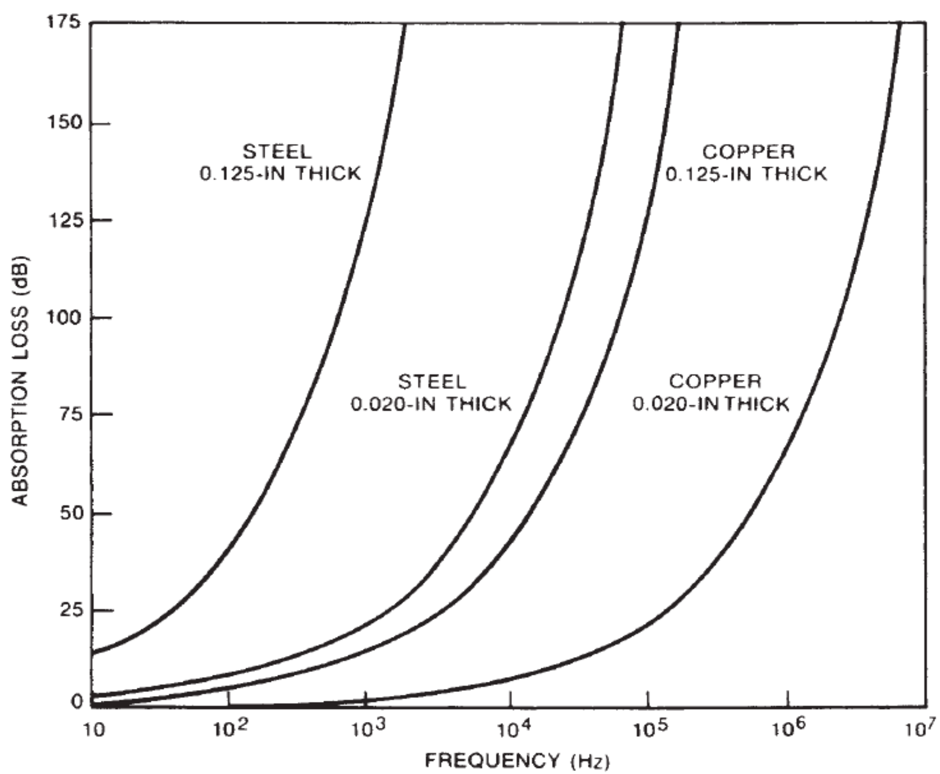

FIGURE 6-9. Absorption loss increases with frequency and with shield thickness; steel offers more absorption loss than copper of the same thickness.

Source : H. W. Ott, Electromagnetic Compatibility Engineering, Wiley, 2009

Shielding of Copper

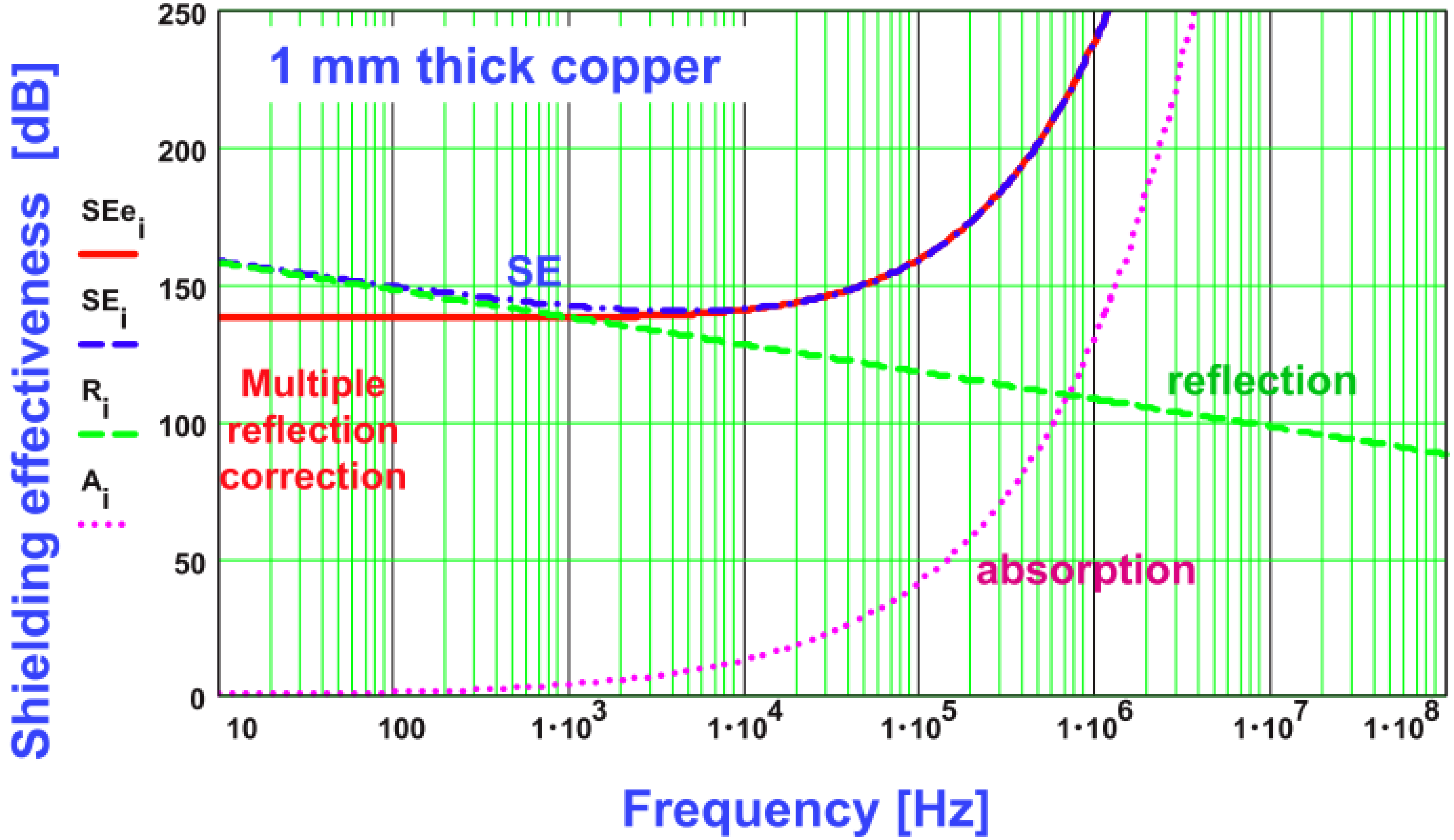

Source : F. Leferink, IEEE EMC Symposium 2010, Fort Lauderdale, Tutorial on EMC Fundamentals; Shielding

Comparison of Copper and Steel

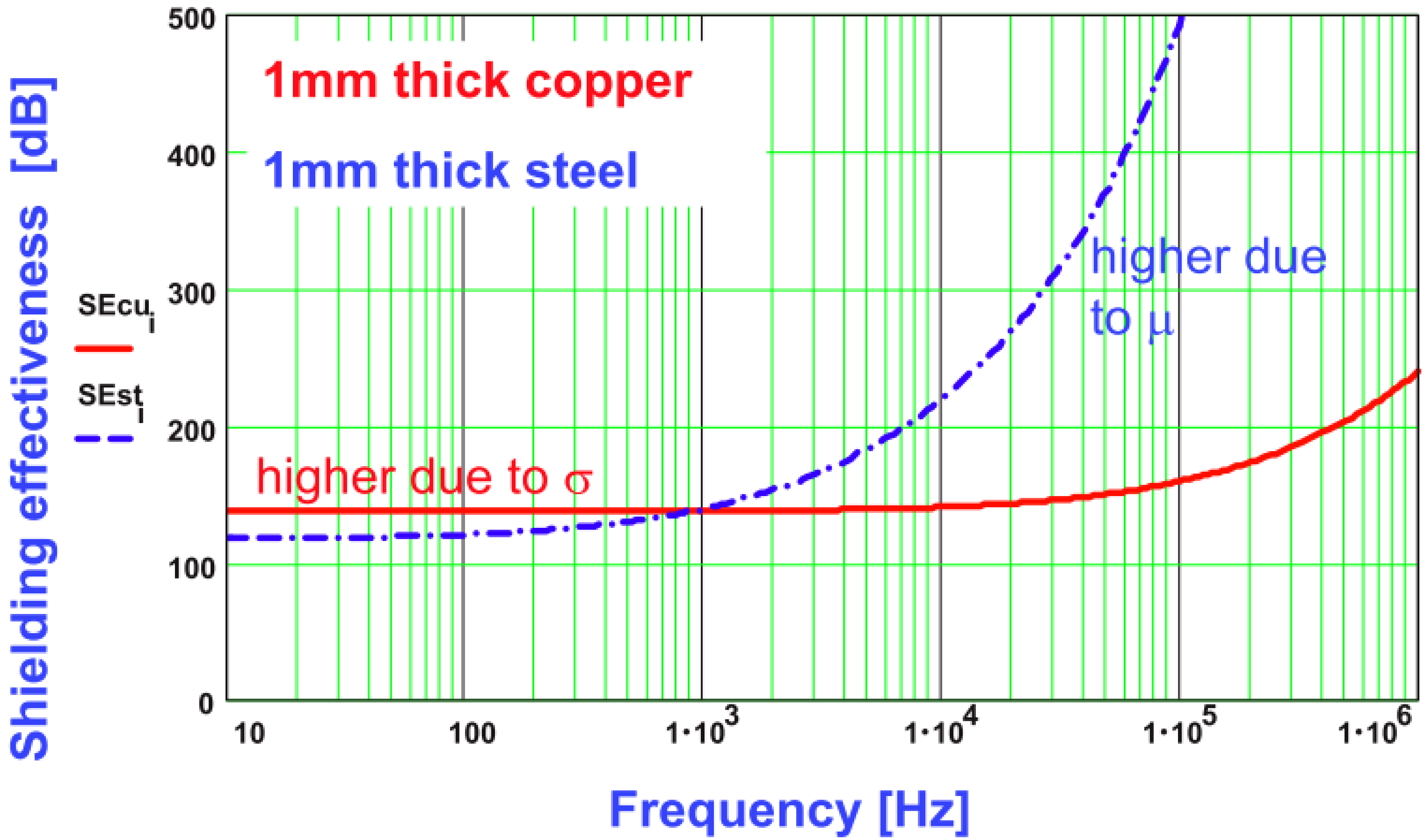

※ Source : F. Leferink, IEEE EMC Symposium 2010, Fort Lauderdale, Tutorial on EMC Fundamentals; Shielding

Near-field Reflection Loss

- Near-field에서 자기장에 대한 전기장의 비는 소스의 특성 임피던스에 크게 의존
  - 높은 전압/낮은 전류 소스 : 파동 임피던스 > 377Ω
  - 낮은 전압/높은 전류 소스 : 파동 임피던스 < 377Ω
- 반사 손실은 파동 임피던스의 함수
  - $R = 20log\frac{|Z_w|}{4|Z_s|}\quad dB$
    - 높은 임피던스 필드 (전기장)는 평면파 보다 높은 반사 손실을 가짐
    - 낮은 임피던스 필드 (자기장)는 평면파 보다 낮은 반사 손실을 가짐

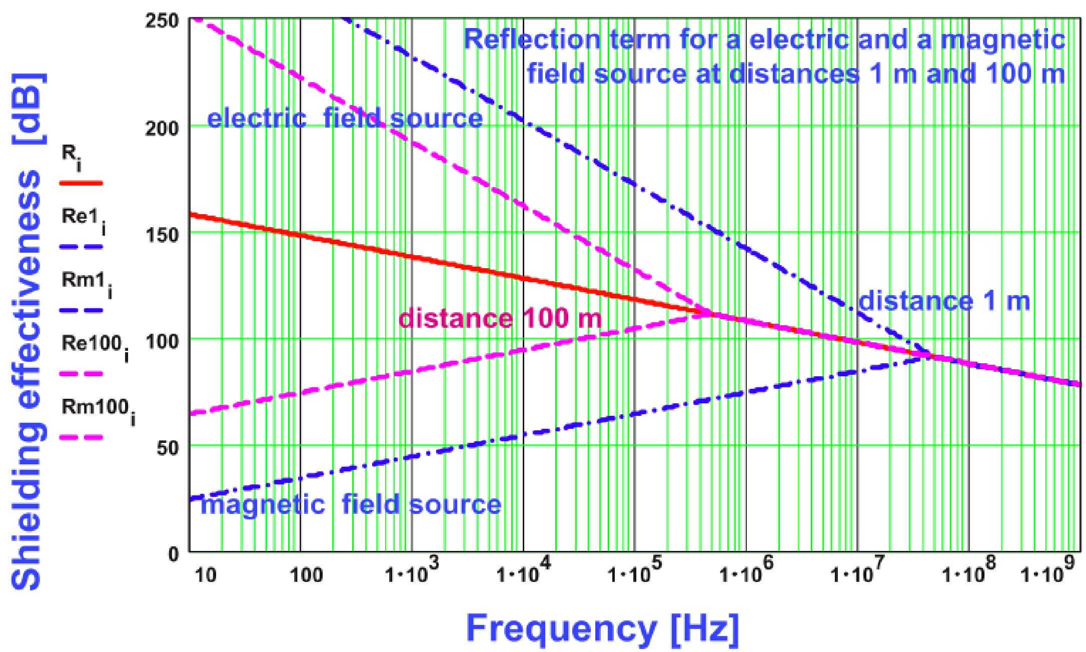

Near-field Reflection Loss

- 전기장 반사 손실
  - 전기장의 점 전원으로 인한 파동 임피던스
    - $|Z_w|_e = \frac{1}{2\pi f \epsilon r}$ (dB) , ($r < \frac{\lambda}{2\pi}$) 여기서 r은 소스에서 쉴드까지 거리(m)
  - 전기장의 반사 손실
    - $R_e = 20log\frac{1}{8\pi f \epsilon r|Z_s|}$ (dB) 혹은 $R_e = 20log\frac{4.5\times10^9}{fr|Z_s|}$ (dB)
    - $R_e = 322 + 10log\frac{\sigma_r}{\mu_r f^3 r^2}$ (dB)

- 자기장 반사 손실
  - 자기장 점 전원으로 인한 파동 임피던스
    - $|Z_w|_m = 2\pi f \mu r$ (dB), ($r < \frac{\lambda}{2\pi}$)
  - 자기장의 반사 손실
    - $R_m = 20log\frac{2\pi f \mu r}{4|Z_s|}$ (dB) 혹은 $R_m = 20log\frac{1.97\times10^{-6} fr}{|Z_s|}$ (dB)
    - $R_m = 14.6 + 10log\left(\frac{fr^2\sigma_r}{\mu_r}\right)$ (dB)

Multiple Reflections in Thin Shield

- **얇은 쉴드에서의 multiple reflection**
  - **만약 쉴드가 얇다면, 두 번째 경계로부터 반사된 파가 첫 번째 경계에서 다시 반사**
  - **그 이후 반사된 파가 두 번째 경계로 되돌아가 다시 반사를 하게 됨**
  - **두꺼운 쉴드의 경우, 흡수 손실이 높기 때문에 무시 가능**

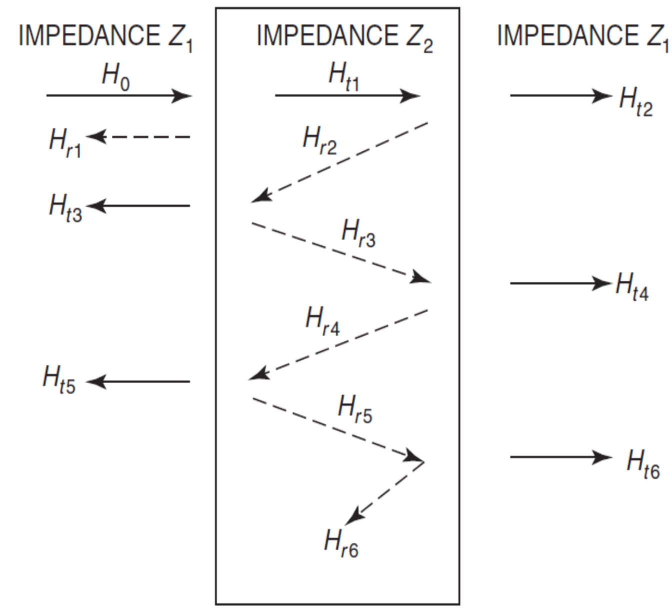

- 전기장의 경우
  - 입사파의 대부분이 첫 번째 경계에서 반사 (적은 비율만 쉴드로 투과)
  - 쉴드 내의 다수 반사는 전기장에 대해서 무시 가능

- 자기장의 경우
  - 입사파의 대부분이 첫 번째 경계에서 쉴드로 투과
  - 투과파의 크기는 입사파 크기의 두 배 (쉴드 내에서 **multiple reflection** 고려 필요)

- 두께가 **t**이고 **skin depth**가 **δ**인 쉴드에서 자기장의 **multiple reflection**에 대한 보정 계수
  - $B = 20log\left(1 - e^{-2t/\delta}\right)\ (dB)$

Source : H. W. Ott, Electromagnetic Compatibility Engineering, Wiley, 2009

Summary : Reflection and Absorption Losses

- 평면파
  - Far field에서 평면파에 대한 전체손실은 흡수손실과 반사손실의 조합이다
  - 평면파에서 다수 반사 보정항은 일반적으로 무시된다
  - 반사손실이 주파수 증가에 따라 감소 – Shield 임피던스가 주파수에 따라 증가
  - 흡수손실은 주파수 증가에 따라 증가 – Skin depth 가 주파수에 따라 감소
  - 저주파에서의 감쇠는 대부분이 반사 손실
  - 고주파에서의 감쇠는 대부분이 흡수 손실

- 전기장
  - 전기장의 경우 반사 손실이 아주 크다
  - 일반적으로 다수 반사 보정 계수는 무시된다
  - 낮은 주파수에서 반사손실은 전기장에 대한 주요 차폐 메커니즘이다.

- 자기장
  - Shield가 두껍다면 (흡수손실 > 9dB) 다수 반사 보정 계수는 무시된다
  - Shield가 얇다면 보정계수는 반드시 포함되어야 한다.
  - Near field에서 저주파 자기장에 대한 반사 손실은 작다.
  - 자기장에 대한 주요 손실은 흡수 손실이다.
  - 흡수손실과 반사손실 모두 저주파에서 작기 때문에, 전체 차폐 효과는 낮기 때문에 저주파 자기장을 차폐하기 힘들다.

Actual Shielding Effectiveness

$$SE = \underbrace{A + R + B}_{\textit{Material Effects}} - \underbrace{\overset{\text{(Slot Effect)}}{\text{Leakage Effects}} - \overset{\text{(Resonance Effect)}}{\text{Standing Wave Effects}}}_{\textit{Structural Effects}}$$

(Diffusion Effect)

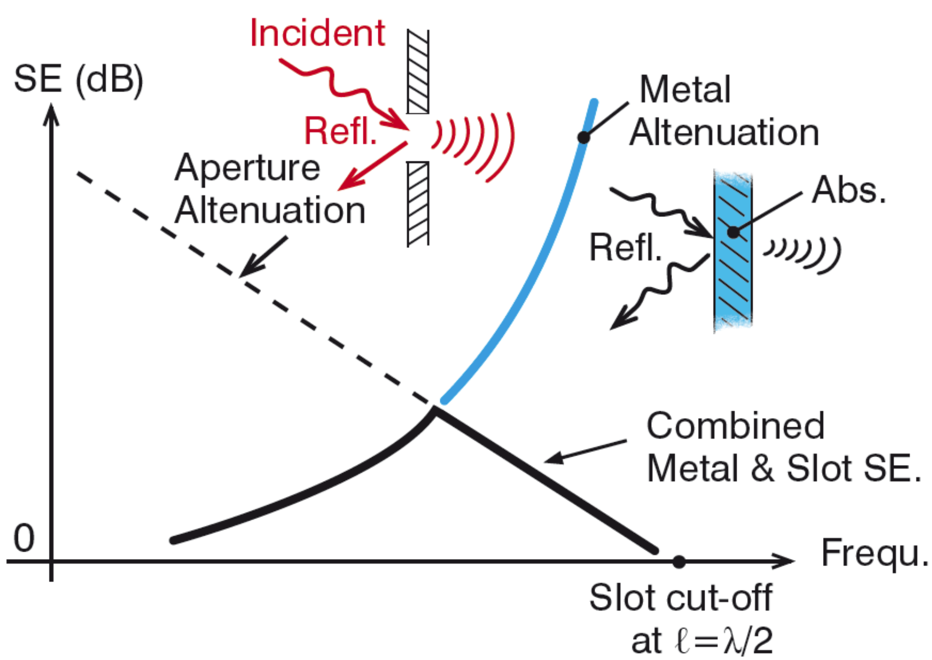

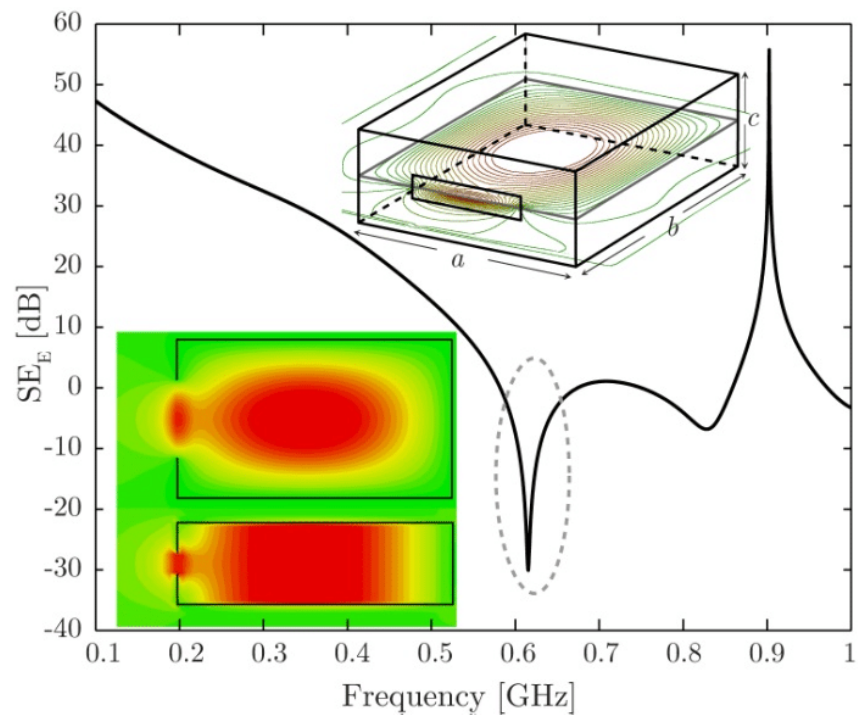

Source : https://www.electronic.nu/2017/02/08/shielding-of-boxes-and-enclosures-part-2/

SE Decomposition

$$\mathrm{SE} = \overbrace{\underbrace{A}_{\substack{\text{Absorption}\\ \text{loss}}} + \underbrace{R}_{\substack{\text{Reflection}\\ \text{loss}}} + \underbrace{B}_{\substack{\text{Multiple}\\ \text{reflections loss}}}}^{\text{Schelkunoff decomposition (terms in dB)}}.$$

$$\mathrm{SE} = L_D + L_M .$$

$$L_M = -10\log_{10}(1 - P_R).$$: mismatch loss

$$L_D = -10\log_{10}(h) \quad h = \frac{P_T}{1 - P_R}$$: dissipation loss

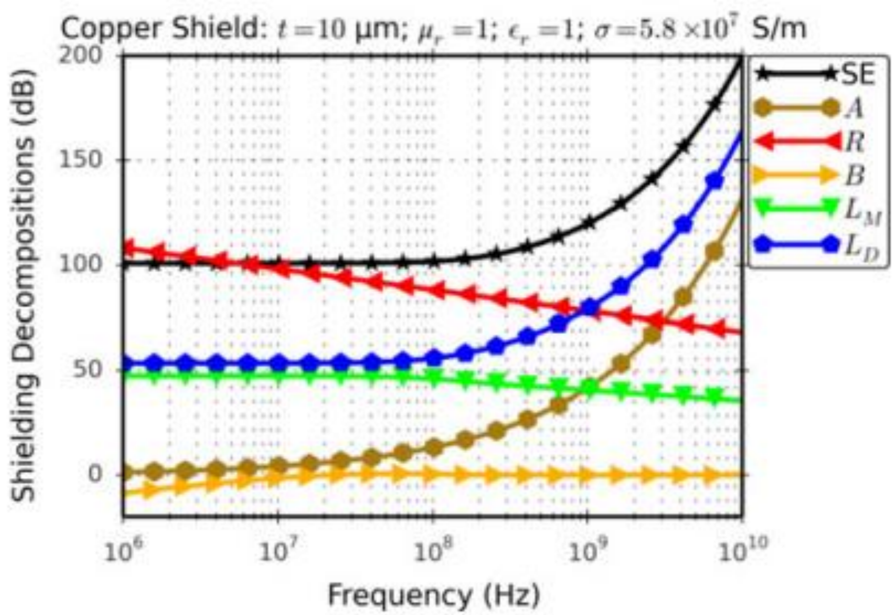

Fig. 1. Shielding decompositions for 10-μm thick copper shield.

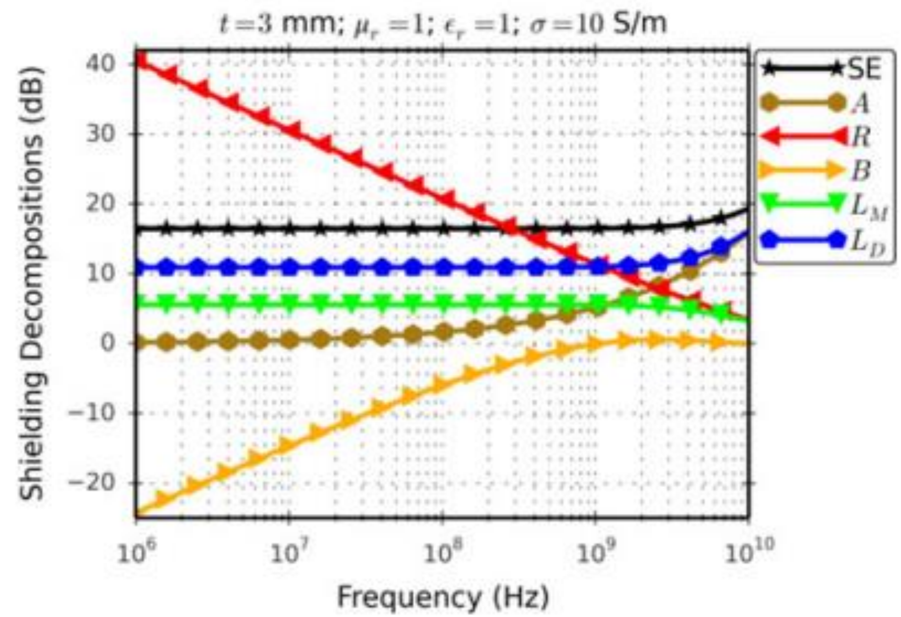

Fig. 3. Shielding decompositions for 3-mm thick shield with $\sigma = 10$ S/m.

Andrew J. McDowell and Todd H. Hubing, "Analysis and Comparison of Plane Wave Shielding Effectiveness Decompositions," IEEE Trans. Electromagn. Compat., vol. 56, no. 6, pp. 1711–1714, Dec. 2014.

원역장 전자파 차폐 측정 기술

Prof. Hyun Ho Park
hhpark@suwon.ac.kr
Dept. Electronic Engineering
The University of Suwon

Far-field SE Measurements

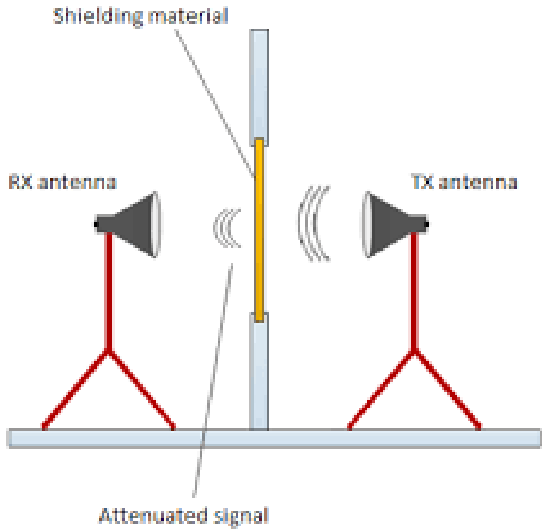

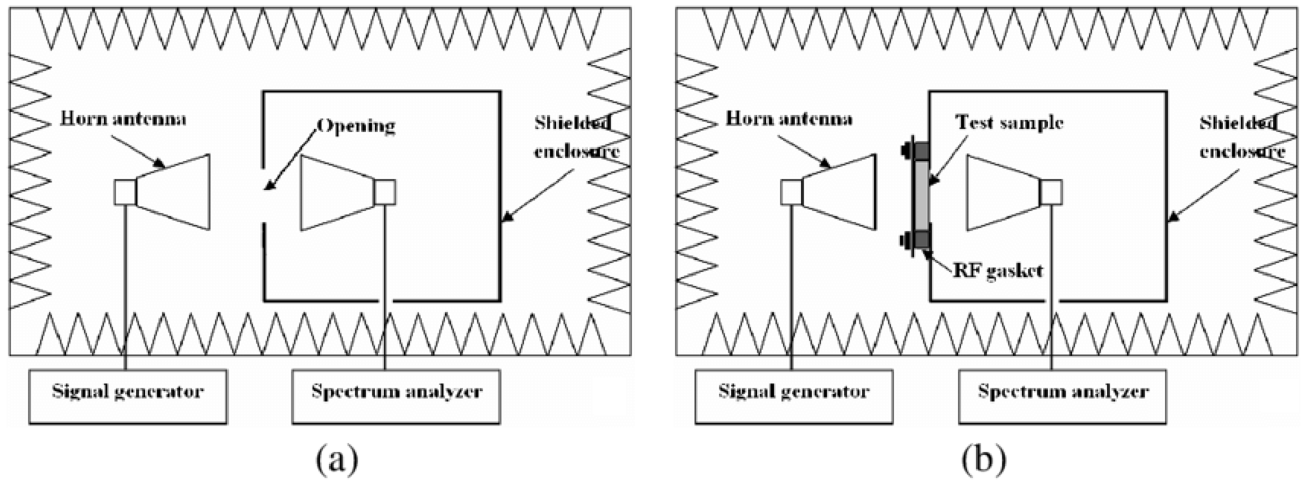

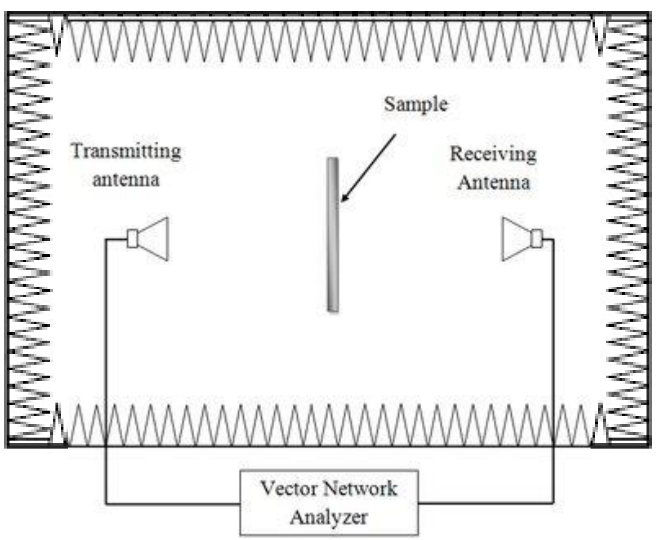

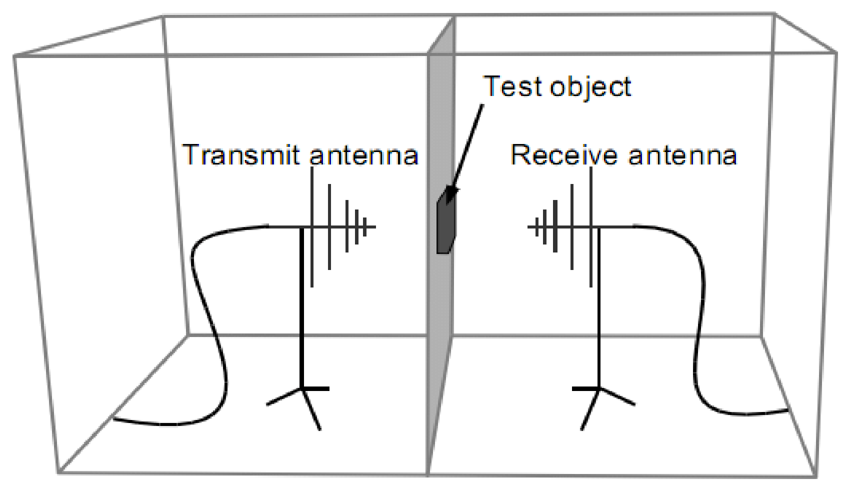

Far-field SE Measurements

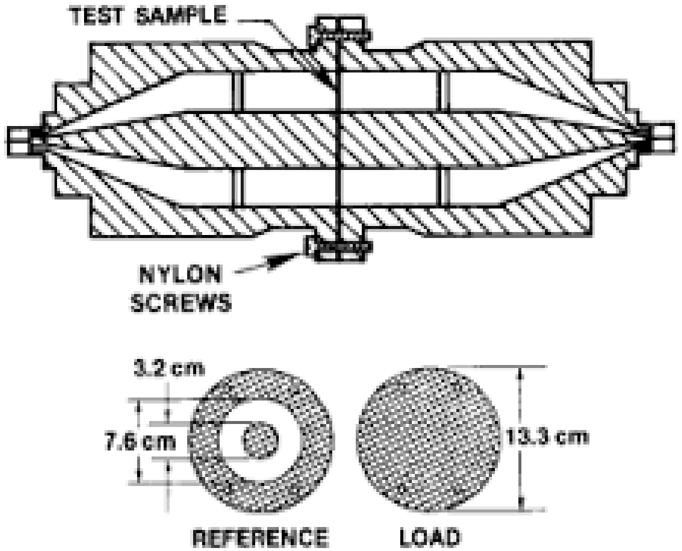

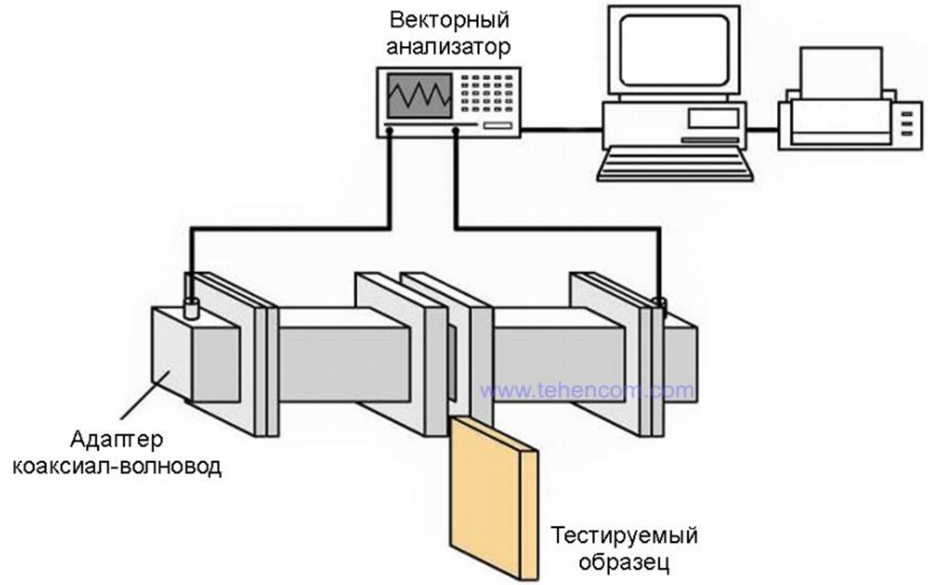

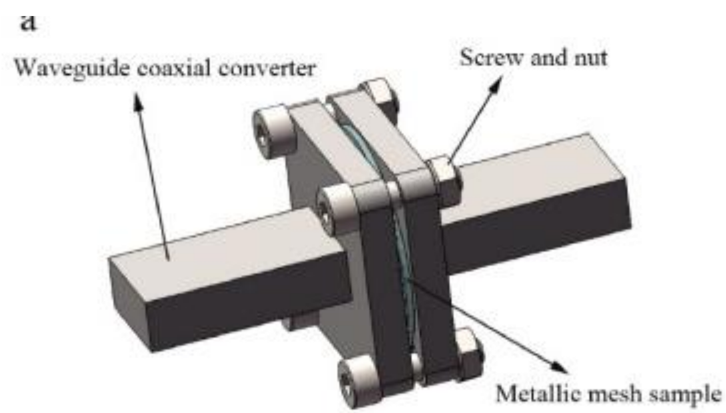

Waveguide는 TEM-mode 전송이 안됨!!!
TM 또는 TE-mode 전송 만 가능함

Far-field SE Measurements Using Coaxial TLs

ASTM-ES7

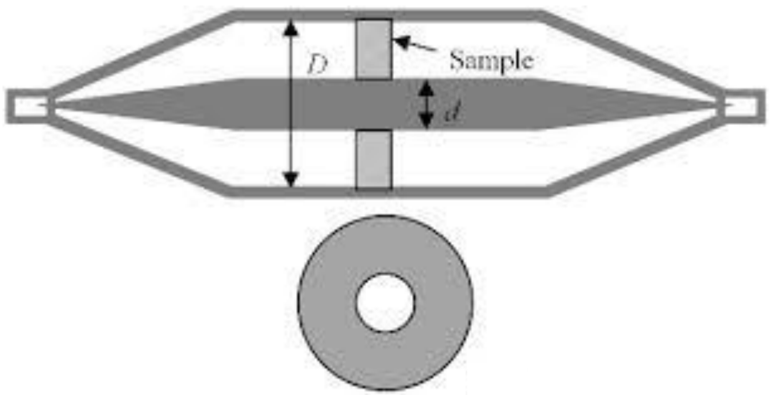

Circular Coaxial
Transmission Line Holder
With Continuous Conductor

ASTM-D4935

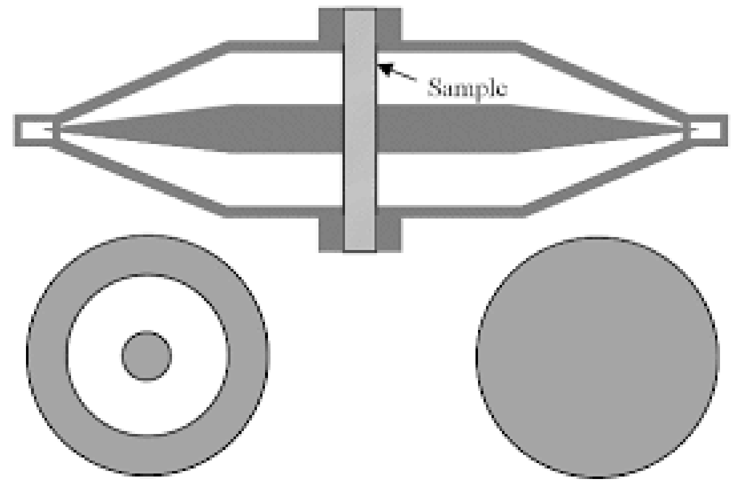

Flanged Circular Coaxial
Transmission Line Holder

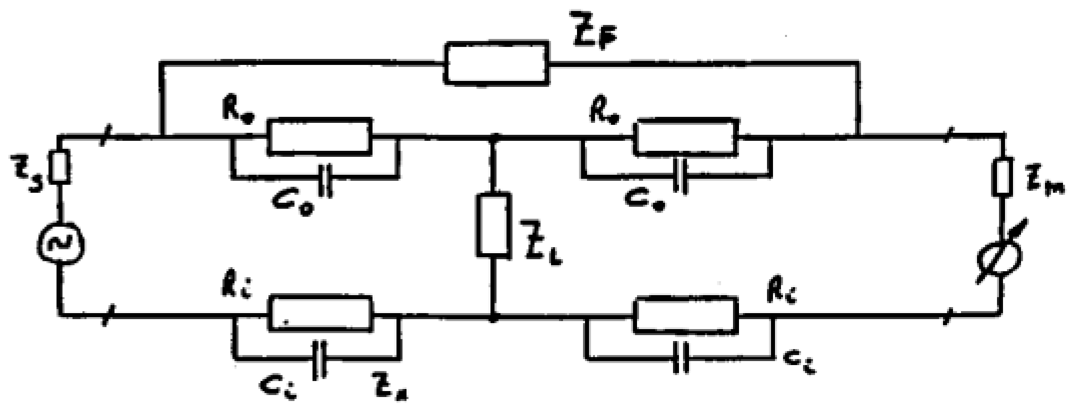

Fig. 2. Common equivalent circuit diagram for TEM-cells.

J. A. Catrysse, M. Delesie, and W Steenbakkers, "The influence of the test fixture on shielding effectiveness measurements," IEEE Trans. Electromagn. Compat., vol. 34, no. 3, pp. 348–351, Aug. 1992.

ASTM-ES7

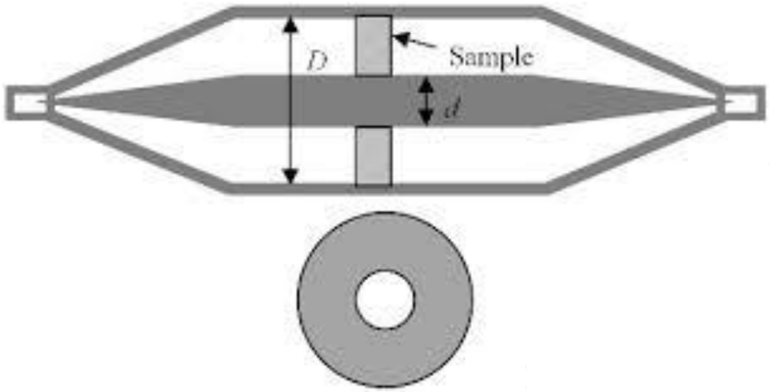

A. ASTM-ES7

The ASTM-ES7 cell was based on a coaxial line, with a continuous conductor. Because of the continuity of both inner and outer conductors, especially Z_f equals zero. This means that all contact impedances are connected in series with the material impedance Z_L. For materials having a good surface conductivity (e.g., metal coated plastics) there is no problem. However, for filled conductive plastics, the contact impedances may be the dominant factor in the whole equivalent impedance. It means that a very careful sample preparation is required, otherwise the measured SE-values may contain significant errors.

To avoid this problem, another measuring technique was proposed.

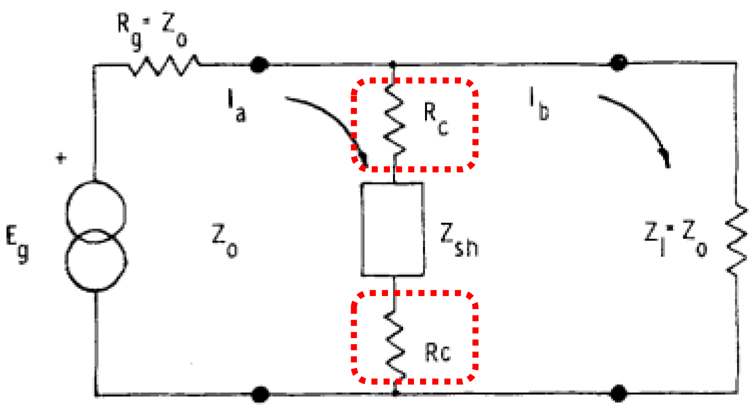

$$IL = 20\log\left|1+\frac{Z_0}{2(Z_L+Z_C)}\right| \xrightarrow{Zc=0} IL = 20\log\left|1+\frac{Z_0}{2Z_L}\right|$$

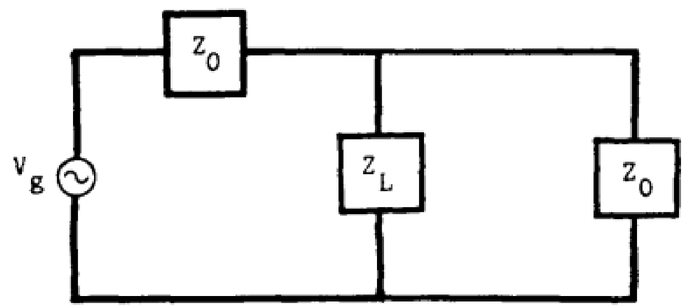

Fig. 5. Idealized coaxial holder transmission-line circuit model.

J. A. Catrysse, M. Delesie, and W Steenbakkers, "The influence of the test fixture on shielding effectiveness measurements," IEEE Trans. Electromagn. Compat., vol. 34, no. 3, pp. 348–351, Aug. 1992.

ASTM-D4935

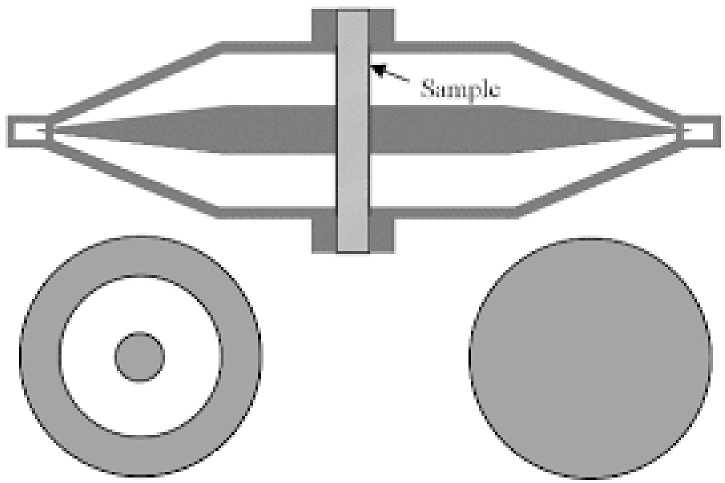

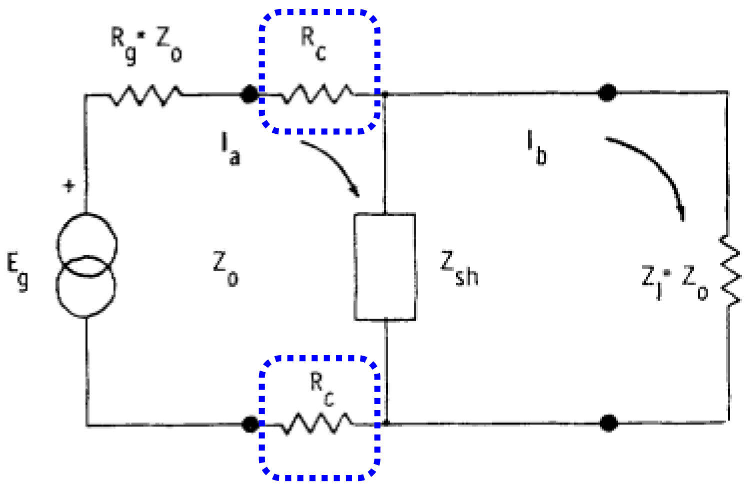

B. ASTM-D4935/89

This cell does not have any continuity for either inner or outer conductors, as can be seen from Fig. 1. Three important types of error can occur when using a noncontinuous, flanged system of measuring cell.

First of all, it is very important to use the cell in a correct way, that is, without making any contact between both parts of the cell, certainly concerning the outer conductor. This means that the outer conductor impedance Z_f should be infinite, otherwise the (capacitive) contact impedances will be in series with the sample impedance X_L and will influence the measured IL-value. To avoid this effect, plastic screws should be used when mounting the sample in the cell, or a nonconductive support should be used for both parts of the cell. It should also be noted that a contact between both parts of the cell may be obtained when holes are drilled through the sample. This is especially the case when carbon powder is used as a filler for the plastic. Fig. 3 shows the effect on the measured SE-value of placing a conductive tape over the ASTM-D4935 cell joint, simulating a good contact between both parts of the cell.

J. A. Catrysse, M. Delesie, and W Steenbakkers, "The influence of the test fixture on shielding effectiveness measurements," IEEE Trans. Electromagn. Compat., vol. 34, no. 3, pp. 348–351, Aug. 1992.

ASTM-D4935

➢ **SE of a Conductive Film Over an Insulating Substrate**

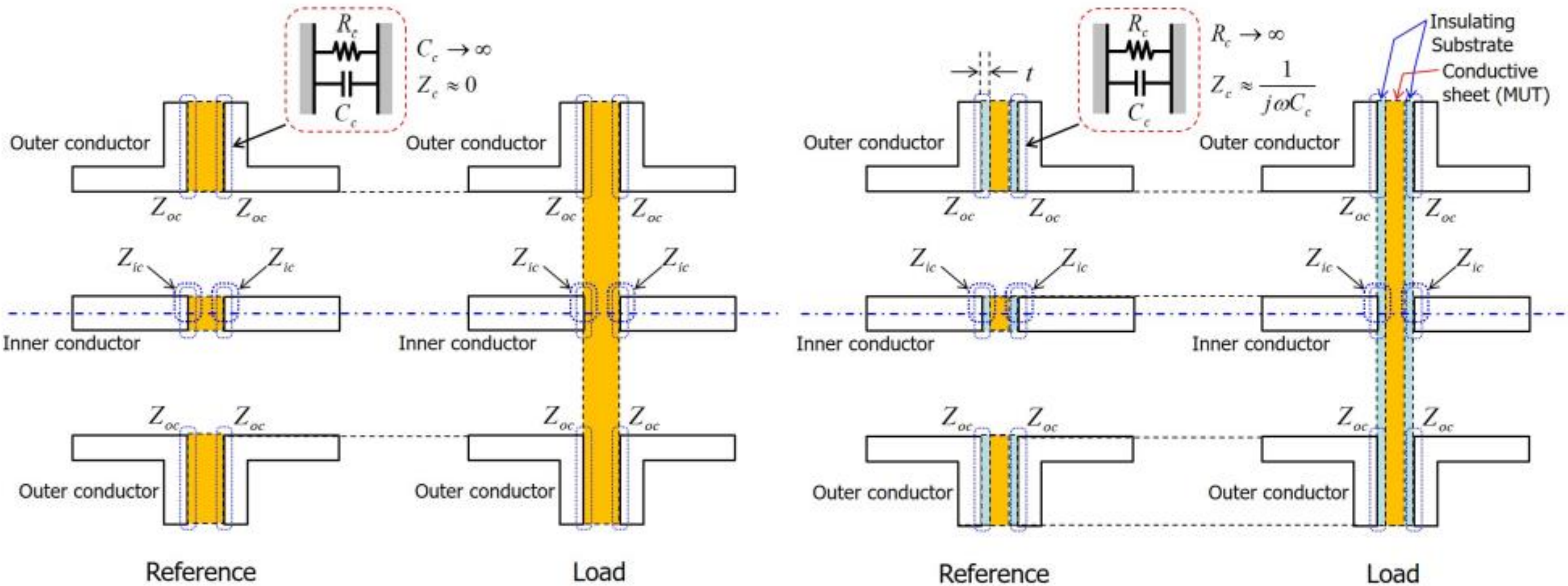

$$SE_0 = 20\log_{10}\left[1 + \frac{Z_0}{2Z_s}\right].$$

$$SE = 20\log_{10}\left|1 + \frac{Z_0 + Z_c}{2Z_s}\right|. \quad \text{(Both-side)}$$

$$SE = 20\log_{10}\left|1 + \frac{Z_0(Z_0 + Z_c)}{Z_s(2Z_0 + Z_c)}\right|. \quad \text{(One-side)}$$

Source : Hyun Ho Park, "Electromagnetic shielding analysis of planar materials using ASTM D4935 standard fixture," *IEEE Trans. Electromagn. Compat.*, vol. 64, no. 5, pp. 1767-1778, Oct. 2022.

ASTM-D4935

➢ Simulation Results

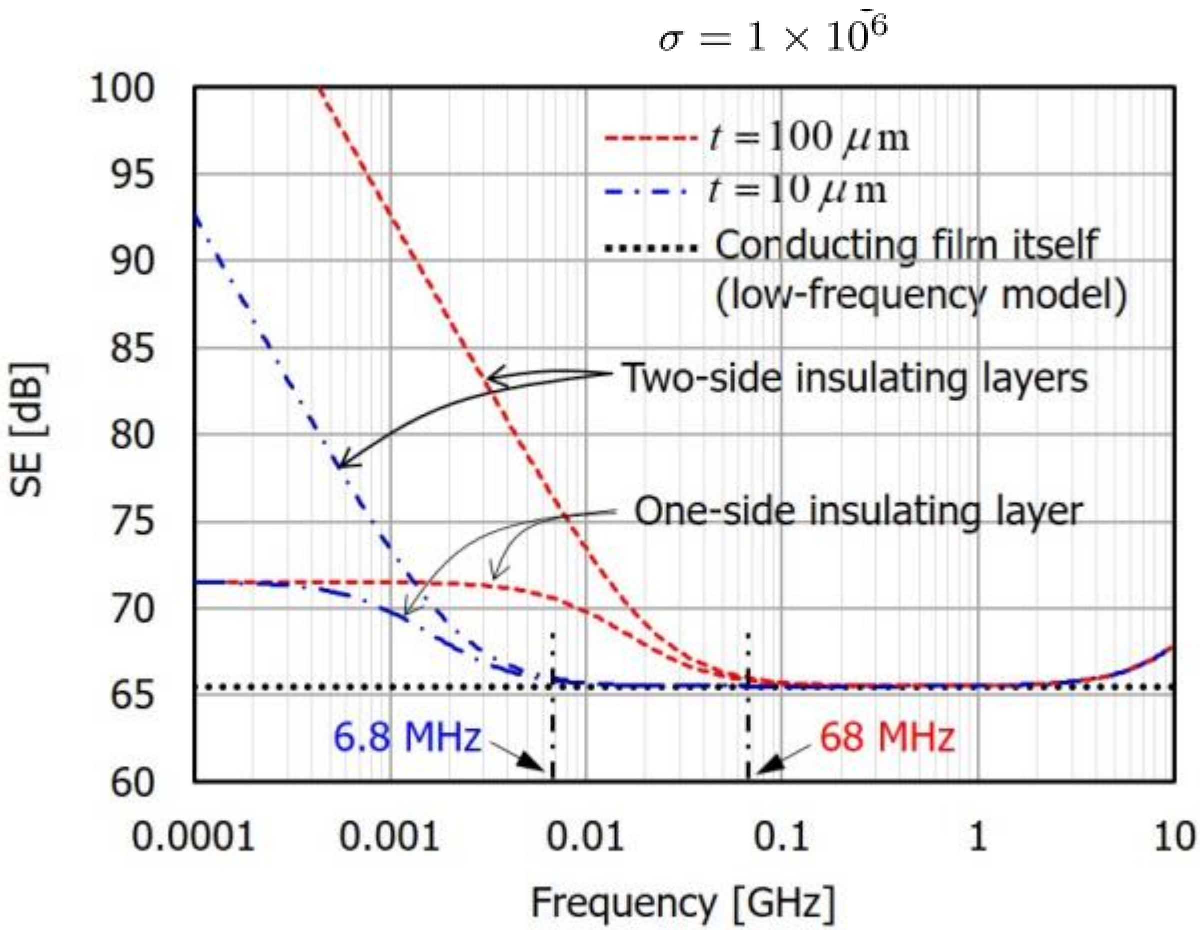

Source : Hyun Ho Park, "Electromagnetic shielding analysis of planar materials using ASTM D4935 standard fixture," *IEEE Trans. Electromagn. Compat.*, vol. 64, no. 5, pp. 1767-1778, Oct. 2022.

ASTM-D4935

➢ Simulation Results

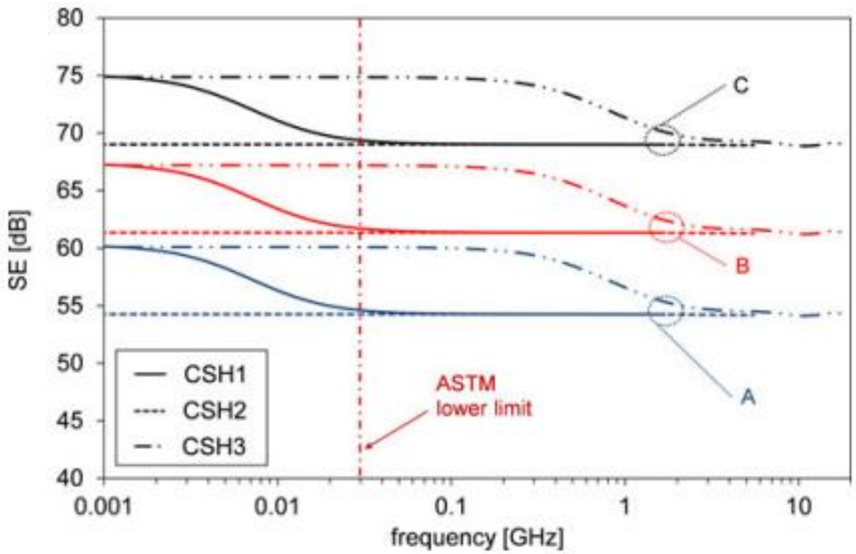

Fig. 9. SE simulations with the equivalent circuit of the CSH1, CSH2, and CSH3 loaded with three different metallic films (A, B, C), which are characterized by a sheet resistance equal to the average of the values reported in Table II.

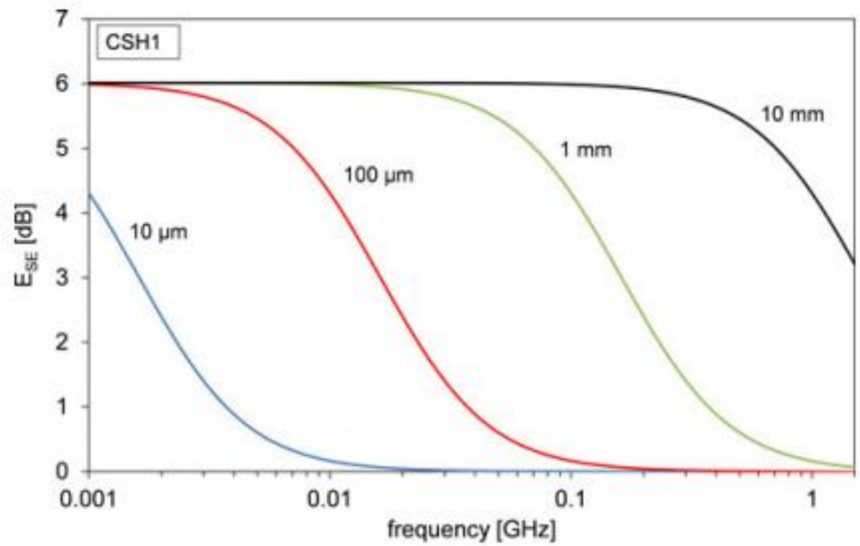

Fig. 10. Difference between the theoretical SE calculated with (9) and the simulated one using the (a) CSH1 and (b) CSH3 equivalent circuits for four different thicknesses of the dielectric substrate ($\varepsilon_r = 2$).

A. Tamburrano, D. Desideri, A. Maschio, and M. S. Sarto, "Coaxial waveguide methods for shielding effectiveness measurement of planar materials up to 18 GHz," *IEEE Trans. Electromagn. Compat.*, vol. 56, no. 6, pp. 1386–1395, Dec 2014.

근역장 전자파 차폐 측정 기술

Prof. Hyun Ho Park
hhpark@suwon.ac.kr
Dept. Electronic Engineering
The University of Suwon

Near-field Sources

➢ **Equivalent Sources on Printed Circuit Boards**

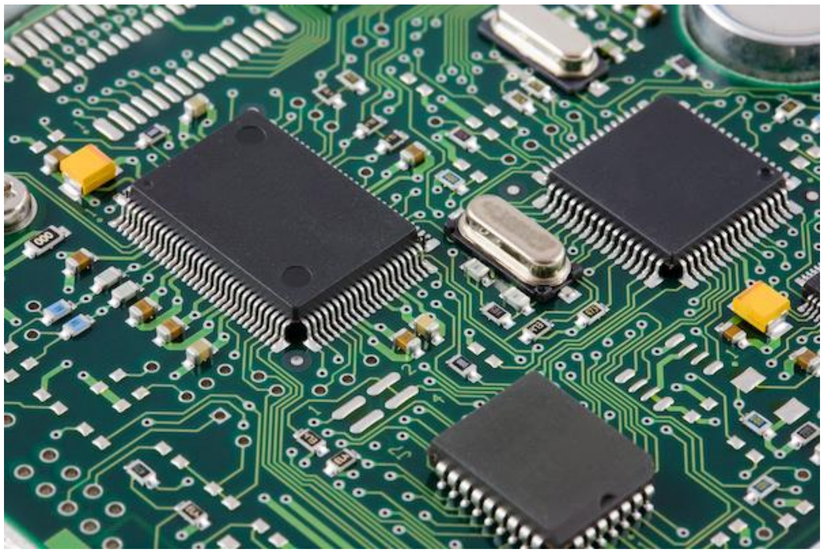

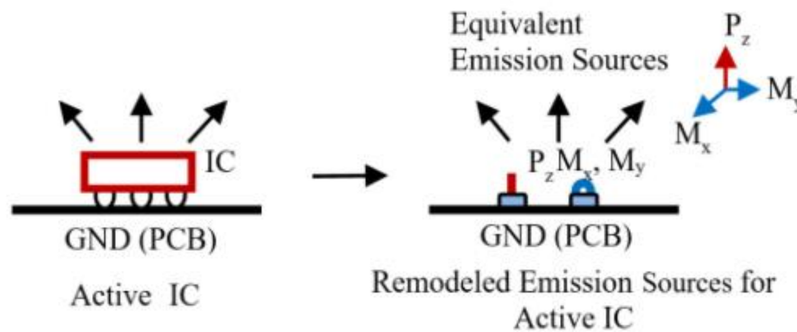

Fig. 2. Equivalent dipole moment model of an active IC.

H. Shrivastav, T. Enomoto, S. Seto, K. Araki, and C. Hwang, Near-Field Scanning-Based Shielding Effectiveness Extraction for Board-Level Shielding Cans, IEEE TRANSACTIONS ON ELECTROMAGNETIC COMPATIBILITY, VOL. 63, NO. 4, AUGUST 2021 pp.1035-1045.

Near-field Sources

➢ **Two Types of Equivalent Sources**

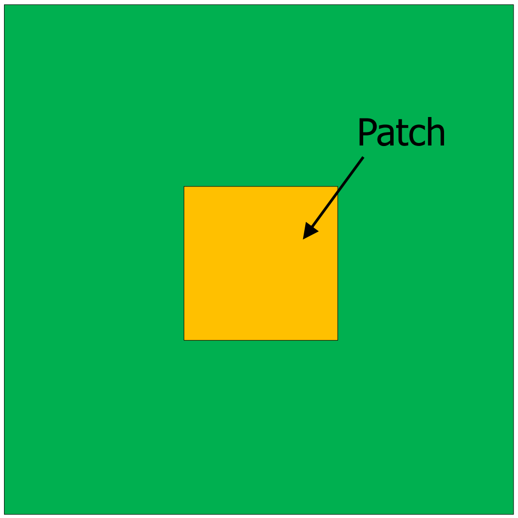

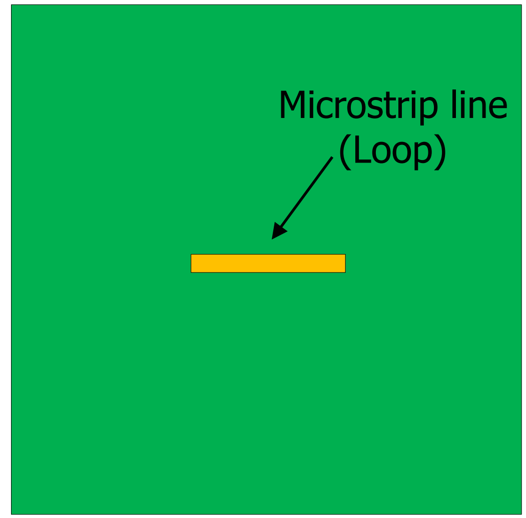

Electric field

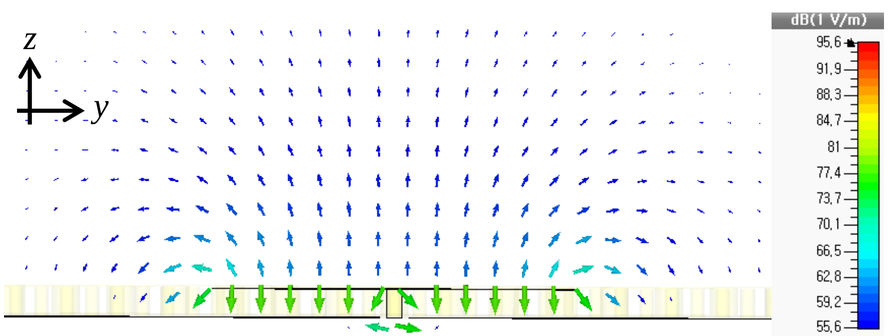

Magnetic field

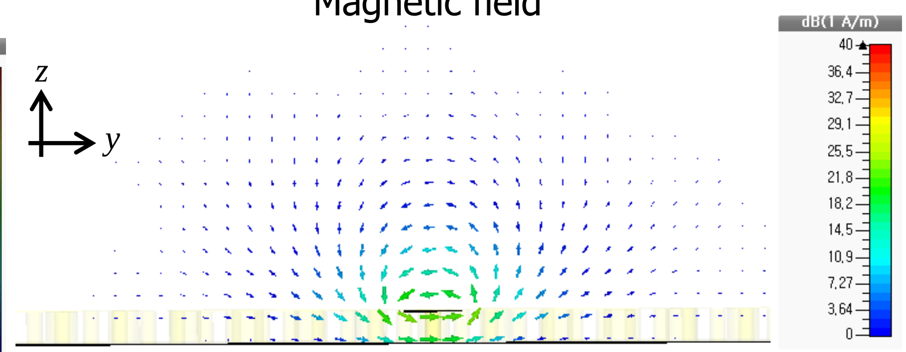

Near-field Sources

➢ **Equivalent Sources on Printed Circuit Boards**

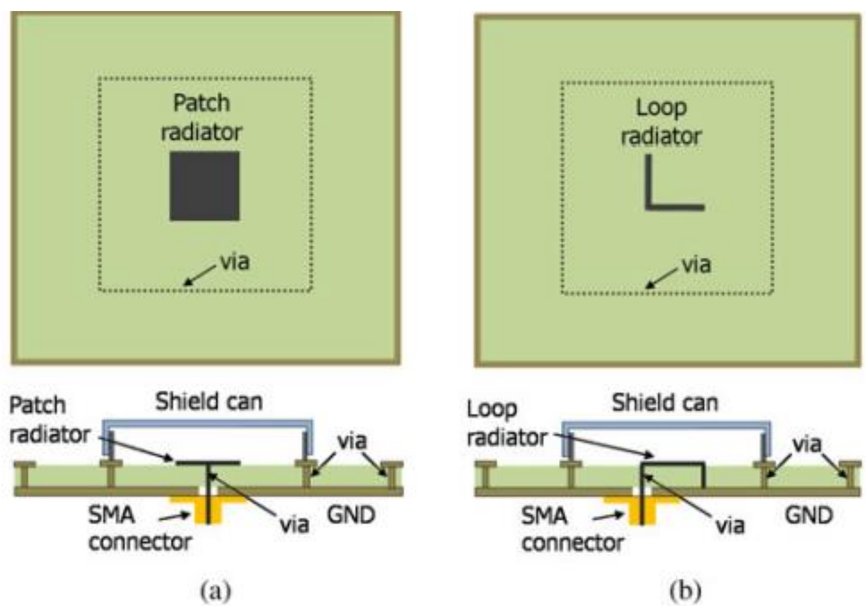

Fig. 3. Configuration of the previous embedded radiators. (a) Patch radiator. (b) Loop radiator.

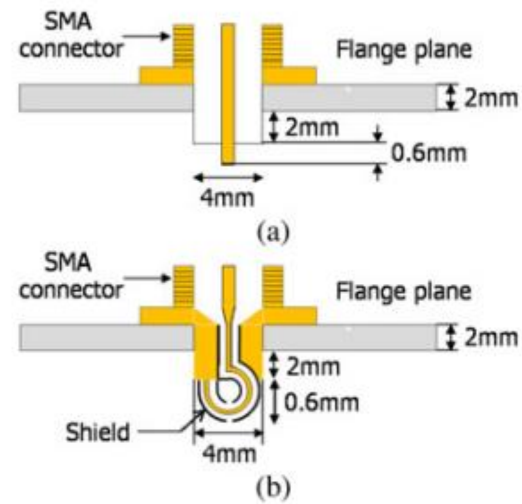

Fig. 5. Configuration of the proposed inserted probes. (a) Monopole probe. (b) Loop probe.

C. Hwang, J.-D. Lim, G. Y. Cho, H.-B. Park, and **H. H. Park**, A Novel Shielding Effectiveness Matrix of Small Shield Cans Based on Equivalent Dipole Moments for Radio-Frequency Interference Analysis, IEEE Trans. Electromagn. Compat., vol. EMC-58, no. 3, pp. 766-775, Jun. 2016.

Near Magnetic-field SE Measurement

- **Loop-probing Method**

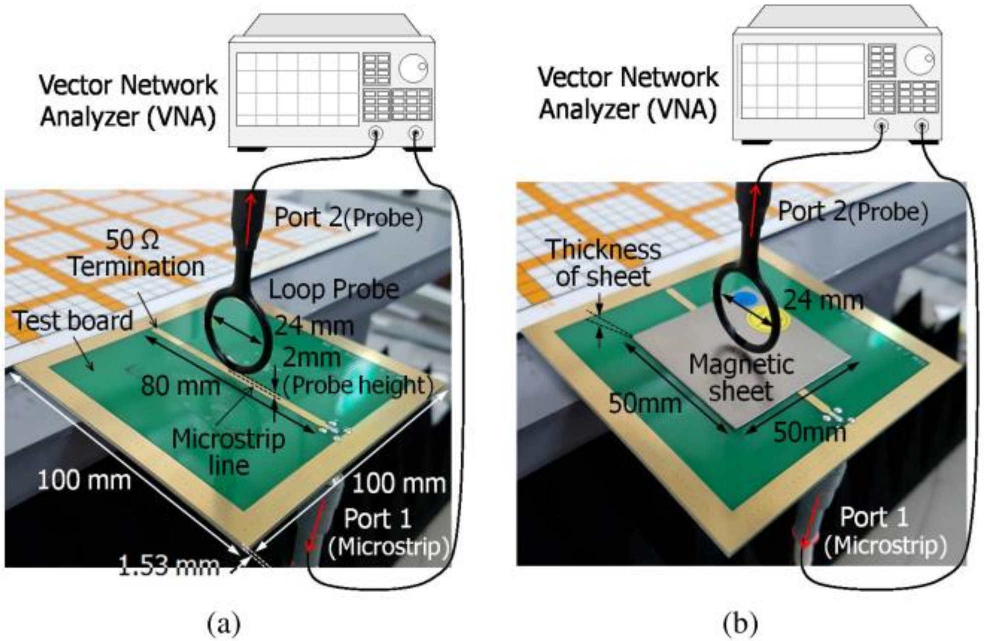

Fig. 1. Shielding measurement setup for magnetic sheets using a microstrip line and a loop probe. (a) Without magnetic sheet. (b) With magnetic sheet.

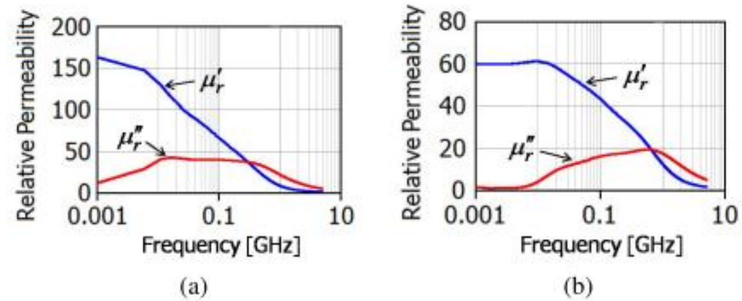

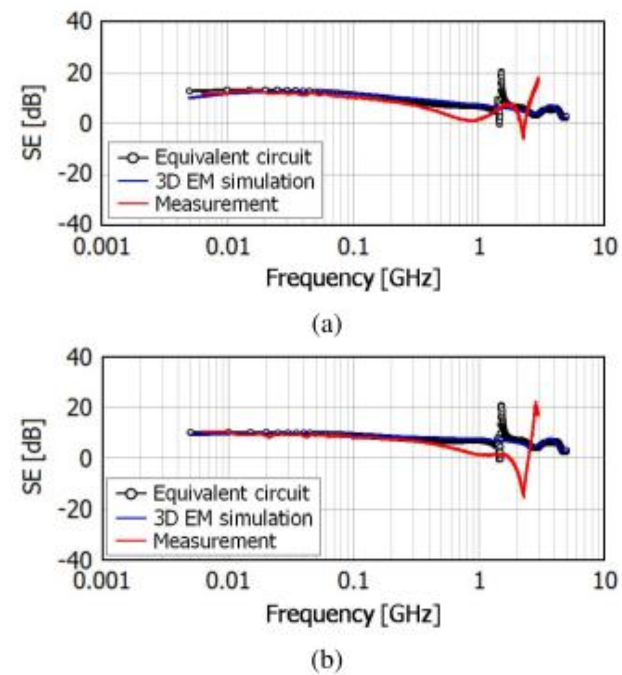

1) **IEC 61967-3**, Integrated circuits - Measurement of electromagnetic emissions - Part 3: Measurement of radiated emissions - Surface scan method, 2014.
2) **Hyun Ho Park**, J. H. Kwon, and S. Ahn, "A simple equivalent circuit model for shielding analysis of magnetic sheets based on microstrip line measurement," *IEEE Trans. Magnetics,* vol. 53, no. 6, Art. ID 9401504, June 2017

Near SE Measurement

- **Dual-TEM Cell Method**

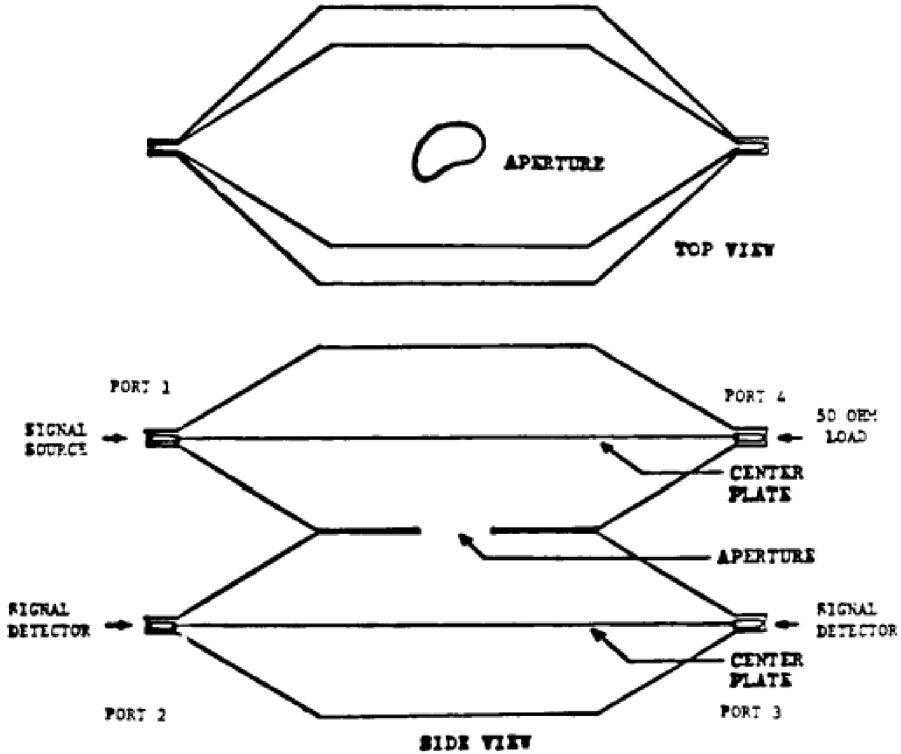

Fig. 1. The dual TEM cell.

Near-field equivalent sources using small apertures

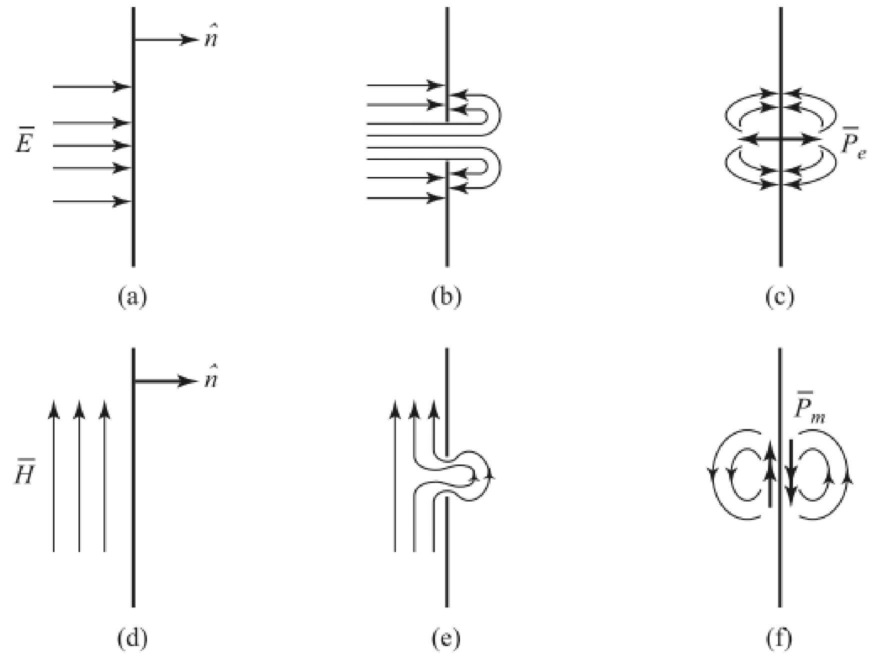

D. M. Pozar, Microwave Engineering, 4th edition, John Wiley & Sons, Inc.

P. F. Wilson and M. T. Ma, Techniques for Measuring the Electromagnetic Shielding Effectiveness of Materials : Part 11-Near-Field Source Simulation, IEEE TRANSACTIONS ON ELECTROMAGNETIC COMPATIBILITY, VOL. 30, NO. 3, AUGUST 1988, pp. 251-259.
P. F. Wilson and M. T. Ma, "Shielding effectiveness measurements with a dual TEM cell," IEEE Trans. Electromagn. Compat., vol. EMC-27, no. 3, pp. 137-142, Aug. 1985.
P. F. Wilson, "A comparison between near-field shielding-effectiveness measurements based on coaxial dipoles and electrically-small apertures," IEEE Trans. Electrornagn. Compat.. vol. EMC-30, no. 1, pp. 123-128, Feb. 1988.

TEM-cell Method (IEC 61967-2)

5.3 Frequency range

The effective frequency range of this radiated emissions procedure is affected by the test cell used. For a 1 GHz TEM cell, the range is 150 kHz to 1 GHz. For a wideband TEM cell (GTEM), the range is 150 kHz to 1 GHz, or as limited by the GTEM and test PCB characteristics.

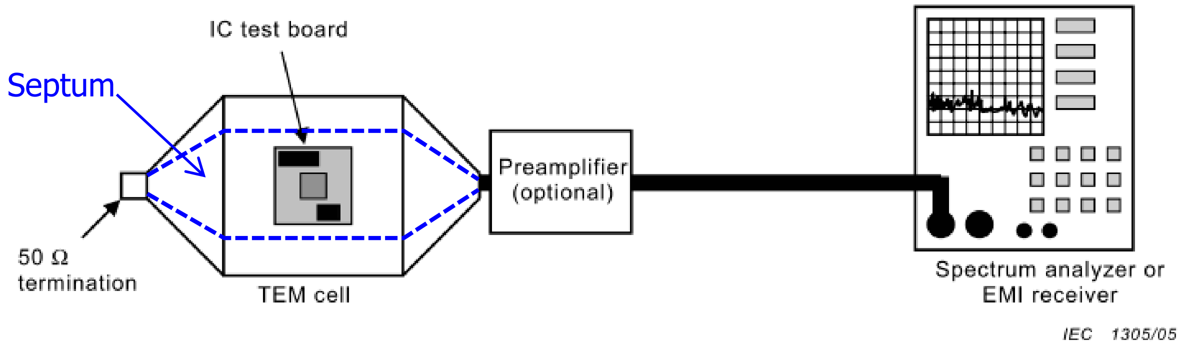

Figure 1 – TEM cell test set-up

Transverse electromagnetic (TEM) cell

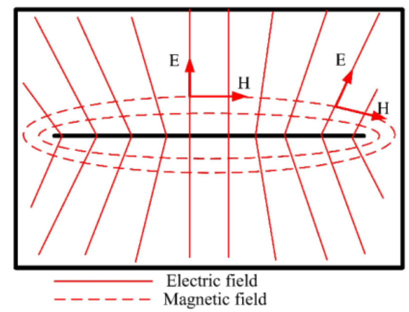

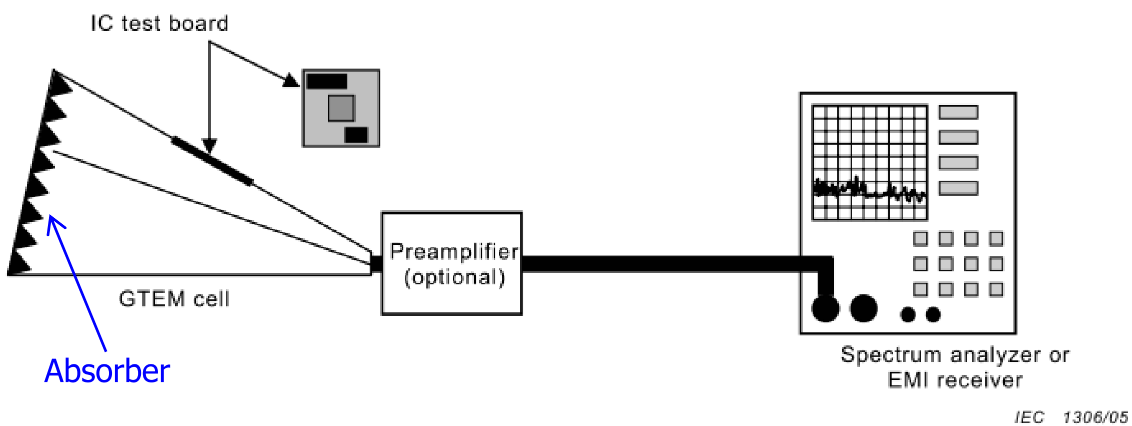

Figure 2 – GTEM cell test set-up

Gigahertz TEM (GTEM) cell

TEM-cell Method (IEC 61967-2)

B.2 Wideband GTEM cell

The wideband TEM cell is an expanded transmission line that does not transition back to a 50 Ω feed as in a conventional TEM cell but continuously expands and is terminated with a septum load and RF absorber material. This cell avoids the moding limitations of conventional TEM cells so that its usable upper frequency is limited not by its dimensions, but by the characteristics of the RF absorber and septum termination. A wideband TEM cell may be almost any practical size with a usable frequency range up to 18 GHz.

While this test method is currently limited to a frequency 1 GHz, wideband GTEM cells offer the potential to extend this limit. An extended frequency limit would be necessary, for example, to enable the proper evaluation of ICs that utilize clock frequencies above 1 GHz. Like any other modification to this test method, the upper frequency limit may be extended as agreed between the manufacturer and user and should be carefully documented in the test report.

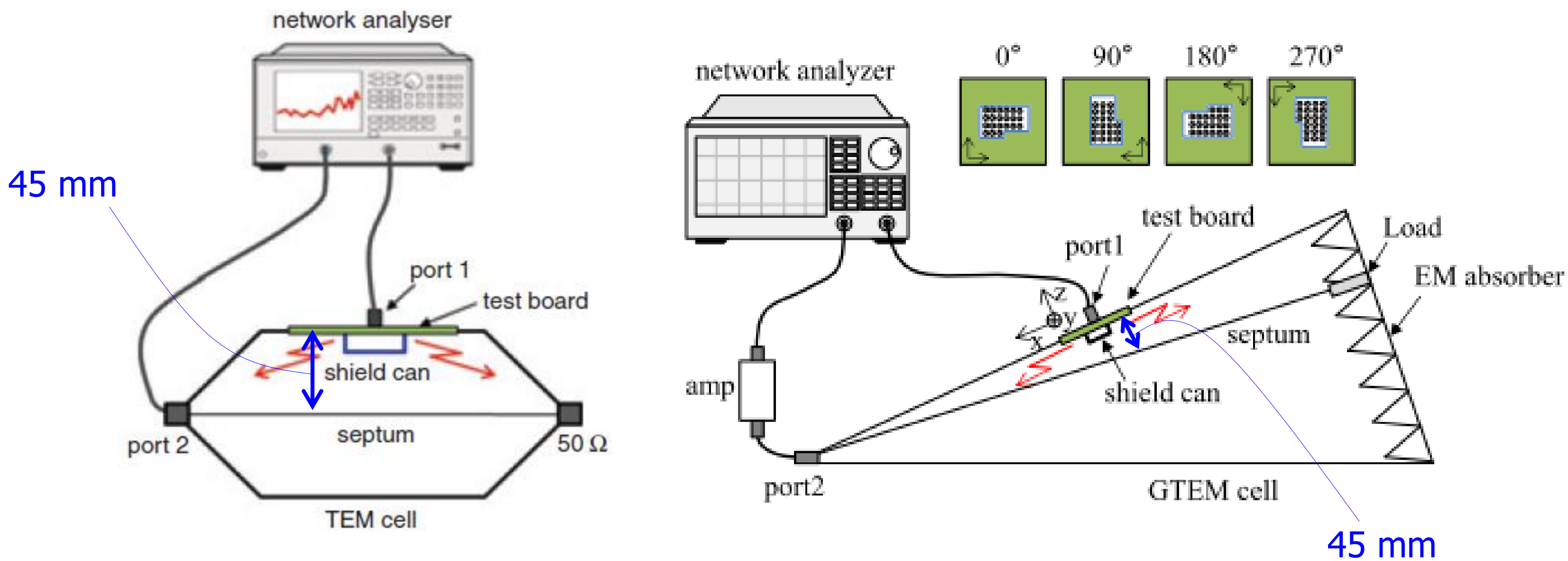

Near SE Measurement

➢ TEM Cell Method

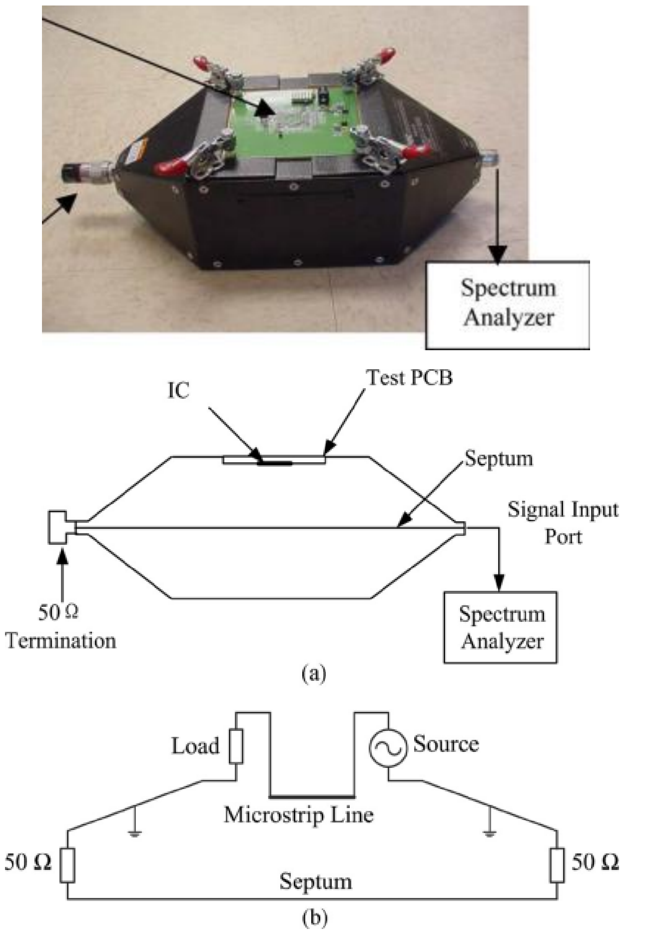

Fig. 1. (a) Standard TEM cell measurement setup and (b) simplified testing model of a microstrip line.

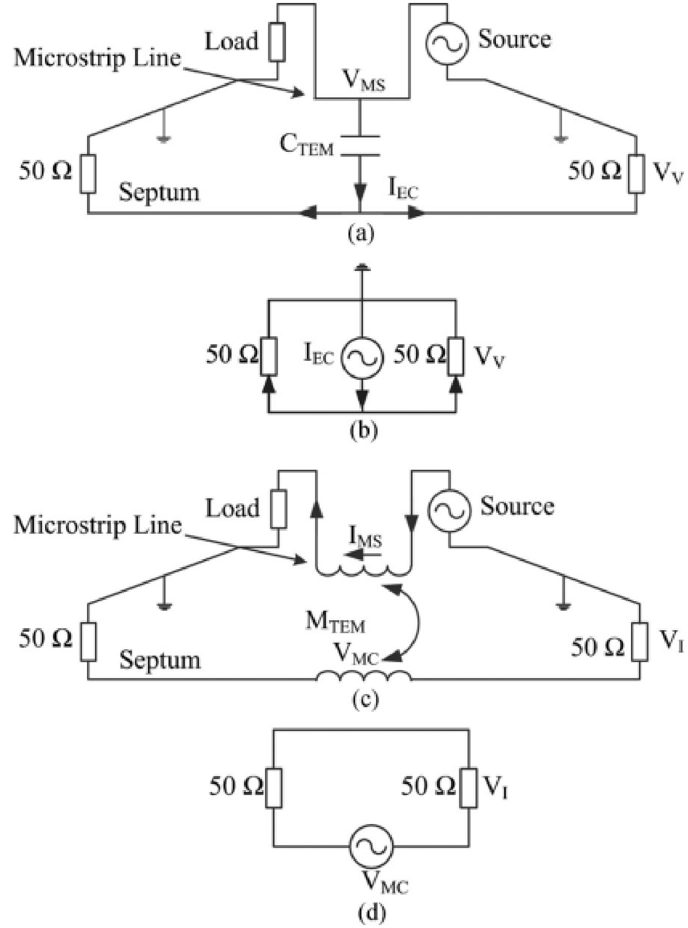

Fig. 2. Equivalent models and circuits for (a), (b) electric and (c), (d) magnetic field couplings between a microstrip line and the septum of TEM cell.

Source : C. Shi, W. Fang, C. Chai, Y. Huang, Y. En, Y. Yang, Y. Liu, Y. Chen, and X. Liao, Using Termination Effect to Characterize Electric and Magnetic Field Coupling Between TEM Cell and Microstrip Line, IEEE Trans. Electromagn. Compat., vol. EMC-57, no. 6, pp. 1338-1344, Dec. 2015.

Extraction of E-coupling and H-coupling

- TEM cell measurements are influenced by both electric and magnetic field coupling from the IC and its package. This paper describes how a TEM cell and a hybrid can be used to isolate electric field coupling from magnetic field coupling. Knowledge of the dominant field coupling mechanism can be used to troubleshoot radiated emissions problems due to ICs.

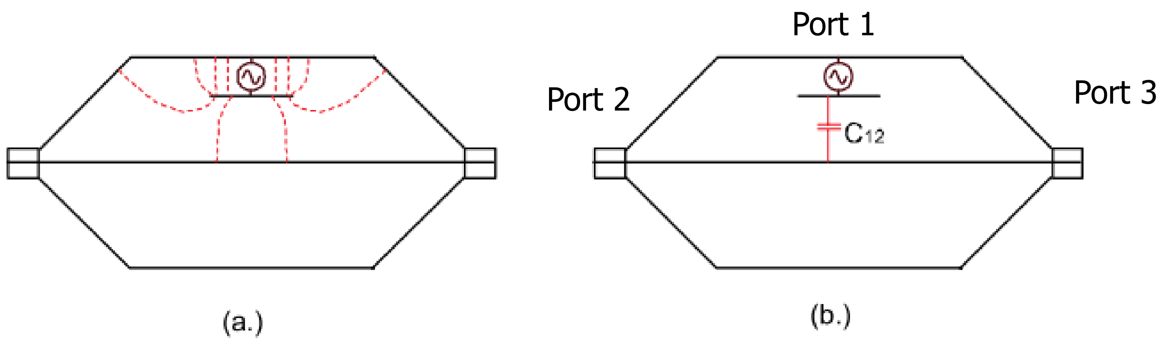

$$O_e = (S_{21} + S_{31})/2.$$

Figure 1. Electric field coupling between a metal patch and a TEM cell.

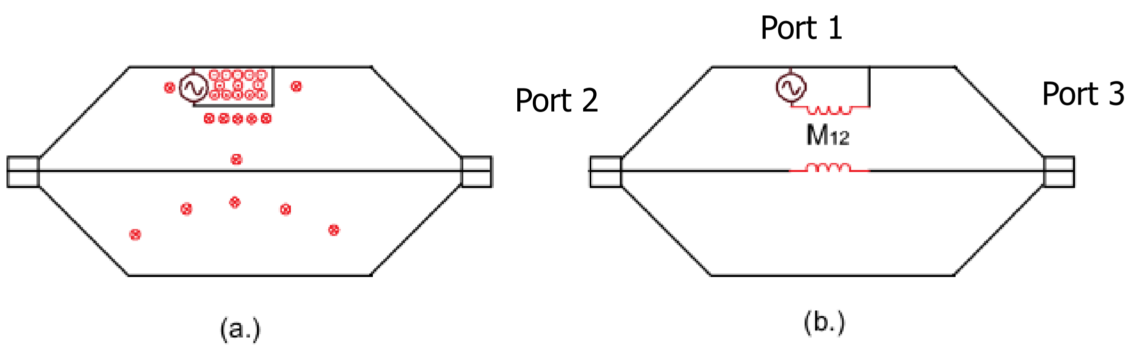

$$O_m = -(S_{21} - S_{31})/2.$$

Figure 2. Magnetic field coupling between a small loop and a TEM cell.

Source : V. Kasturi, S. Deng, T. Hubing and D. Beetner, "Quantifying Electric and Magnetic Field Coupling from Integrated Circuits with TEM Cell Measurements", 2006 IEEE International Symposium on Electromagnetic Compatibility, 14-18 Aug. 2006.

Extraction of E-coupling and H-coupling

➢ **With a Hybrid**

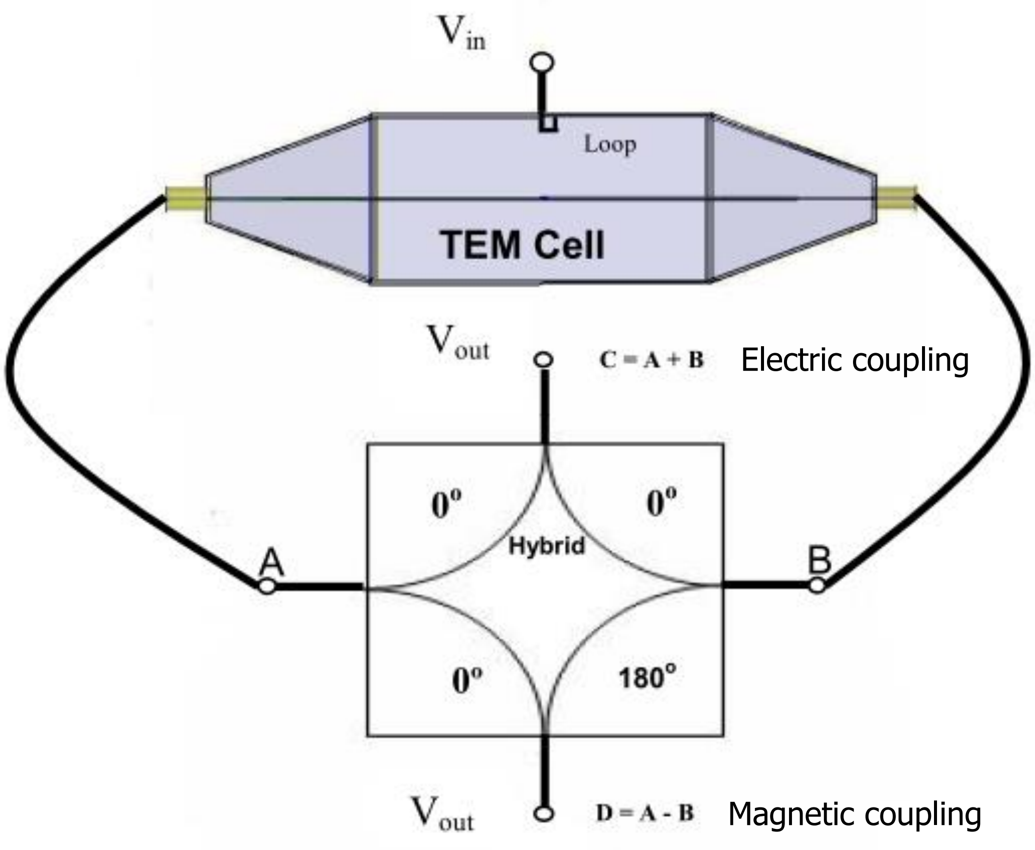

Figure 3. TEM cell with hybrid.

Source : V. Kasturi, S. Deng, T. Hubing and D. Beetner, "Quantifying Electric and Magnetic Field Coupling from Integrated Circuits with TEM Cell Measurements", 2006 IEEE International Symposium on Electromagnetic Compatibility, 14-18 Aug. 2006.

Near SE Measurement

➢ **TEM Cell Method**

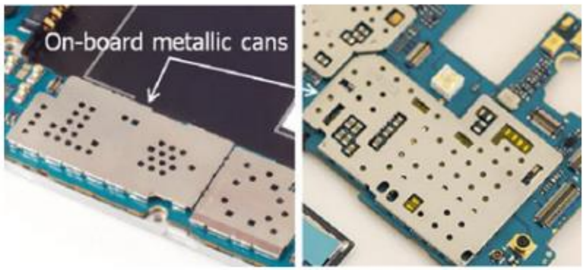

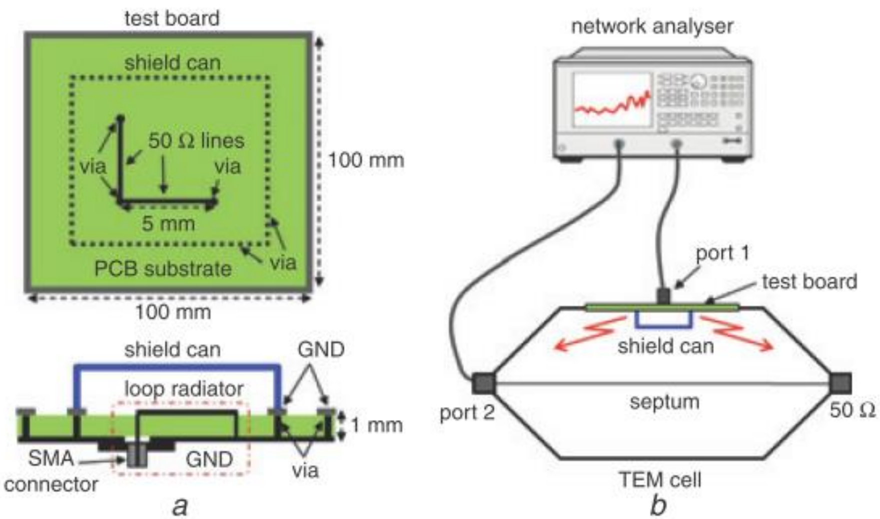

Fig. 2 *Proposed shielding measurement method for small shield cans*
a Configuration of test board with L-shaped radiator pattern
b Shielding measurement setup using TEM cell

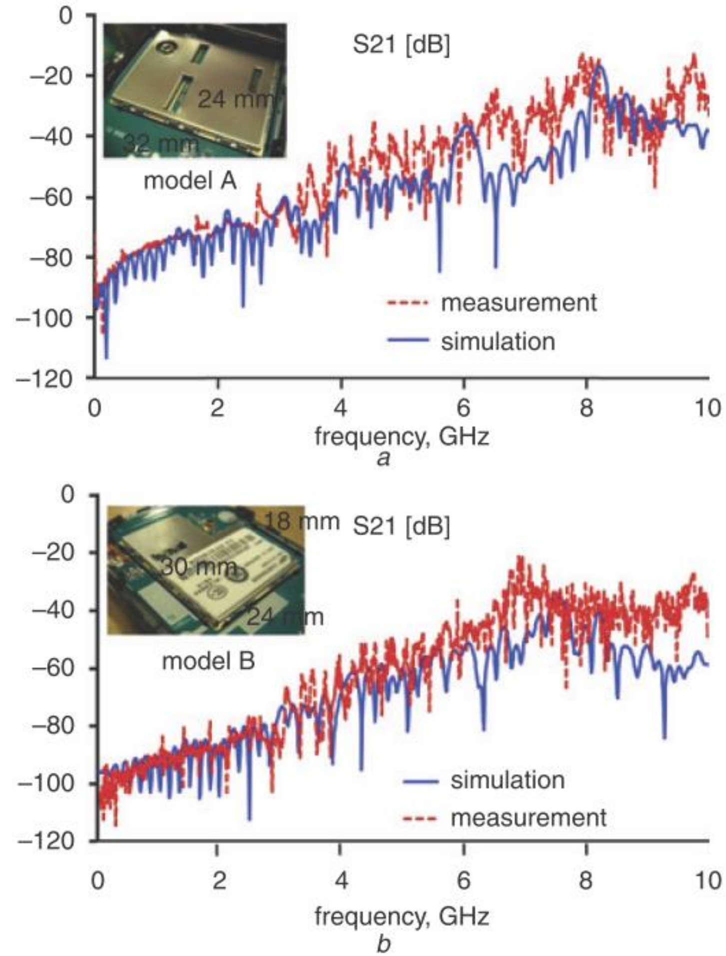

Fig. 5 *Comparison of measured and simulated S_{21} of two real shield cans*
a Model A
b Model B

Source : **H. H. Park**, Simple shielding evaluation method of small shield cans on printed circuit boards in mobile devices, ELECTRONICS LETTERS 18th July 2013 Vol. 49 No. 15.

IC-Stripline Method (IEC 61967-8)

IEC 61967-8

Edition 1.0 2011-08

INTERNATIONAL STANDARD

NORME INTERNATIONALE

colour inside

Integrated circuits – Measurement of electromagnetic emissions –
Part 8: Measurement of radiated emissions – IC stripline method

Circuits intégrés – Mesure des émissions électromagnétiques –
Partie 8: Mesure des émissions rayonnées – Méthode de la ligne TEM à plaques (stripline) pour CI

IC-Stripline Method

➢ Test Configuration : Radiated Emission

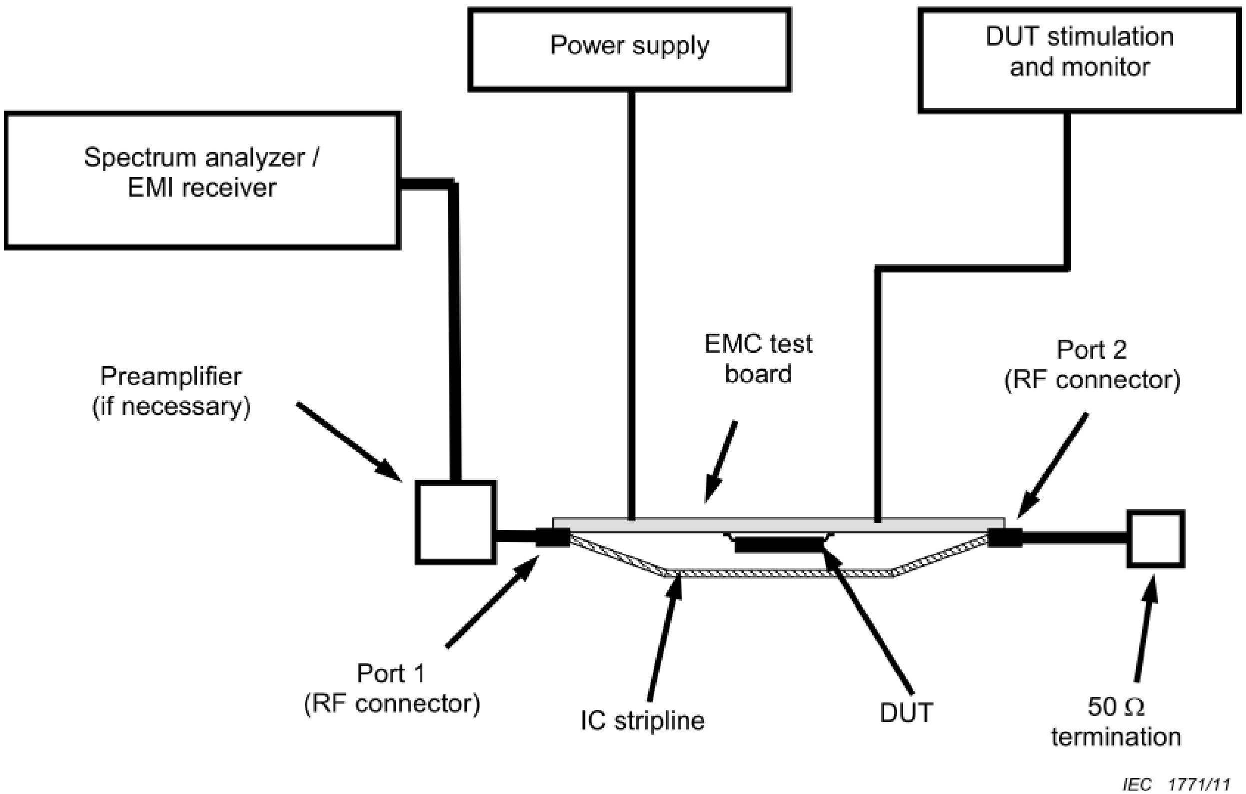

Figure 1 – IC stripline test set-up

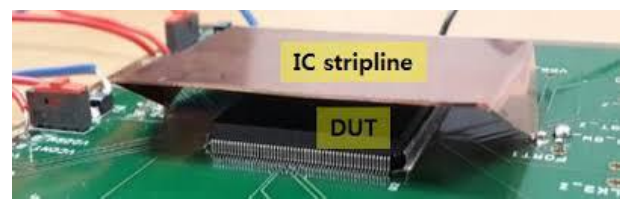

Near Magnetic-field Measurement

- **Strip-line Method**

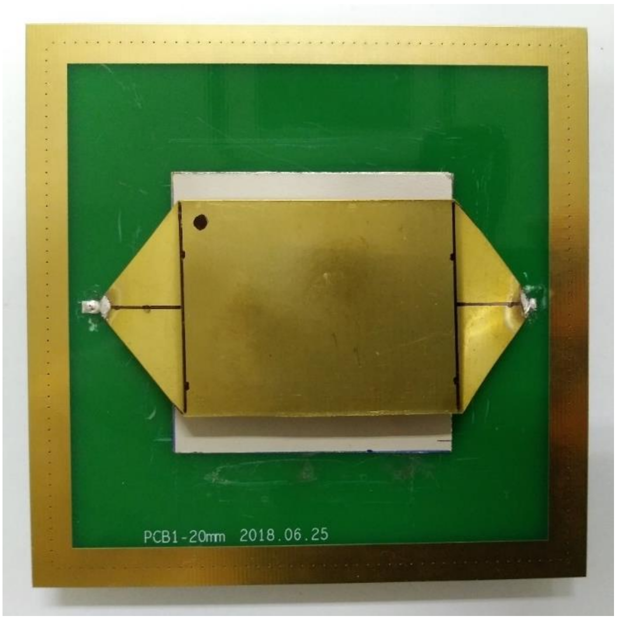

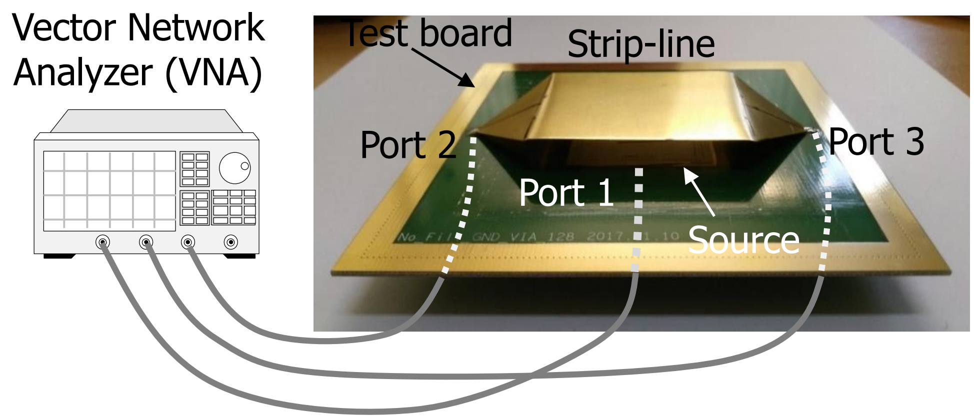

1) **IEC 61967-8**: Integrated circuits - Measurement of electromagnetic emissions - Part 8: Measurement of radiated emissions - IC stripline method , 2011.
2) **Hyun Ho Park**, G. Seo, Y. K. Kwon, and H.-B. Park "Shielding evaluation of on-package conformal shields by numerical modeling and experimental measurement," *Electronics Letters*, vol. 53, no. 14 pp. 916–918, 6th July 2017.

IC-Stripline Method

➢ Design of Stripline

A.3 Conversion for different active conductor heights

A conversion factor (X) to correlate measuring results of IC striplines with different heights to the default IC stripline height of 6,7 mm can be calculated by:

$$X = 20 \times \lg\left(\frac{h_1}{h_2}\right) \quad \text{(A.2)}$$

where

X is the conversion factor (dB) to IC stripline 6,7 mm height type results;

h_1 is the active conductor height of specific type;

h_2 is the active conductor height of 6,7 mm type .

For example the conversion factor for a 8 mm IC stripline is X = 1,54 dB. That means 1,54 dB has to be added to the measured voltage in dBµV at the measurement port of the 8 mm height IC stripline.

IC stripline sensitivity is higher than GTEM cell sensitivity
(results ~19 dB higher for 5 mm and ~16 dB for 6.7 mm IC stripline compared to GTEM)

Commercial IC Stripline

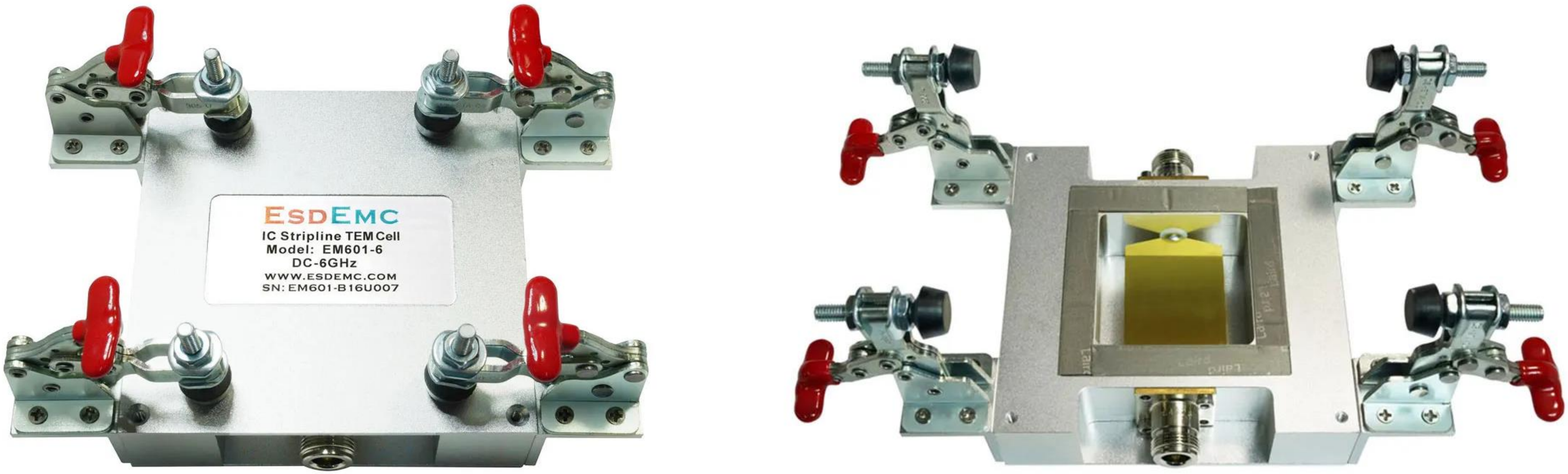

EM601-6 IC Stripline TEM Cell (DC-6 GHz, 5kV Pulse)

EM603-8 IC Stripline TEM Cell (DC-8 GHz, up to 1 kV)

https://www.esdemc.com/products/emc-rf-solutions/em601-6/

IEC 62333

➢ **Noise suppression sheet for digital devices and equipment**

INTERNATIONAL STANDARD

IEC 62333-1

First edition
2006-05

Noise suppression sheet for digital devices and equipment –

Part 1:
Definitions and general properties

경청해 주셔서

감사합니다!